Measurement Notes

Note 55

Impulse Propagation Measurements of the Dielectric Properties of Several Polymer Resins

W. Scott Bigelow
Everett G. Farr
Farr Research, Inc.

November, 1999

Abstract

We measured the complex permittivity of materials for potential use in constructing graded-layer dielectric transmission line bends. For comparison, we also measured the dielectric constant of ultra-high-molecular-weight polyethylene. The procedure, described in Measurement Notes 49 and 52, depends on a comparison of impulse transmission through two different lengths of material embedded in a coaxial test fixture. We cast samples of several polyurethane formulations, some of which included titanium dioxide powder to adjust the dielectric properties. We also measured the dielectric constant of polystyrene loaded with titanium dioxide, supplied by a manufacturer of microwave dielectric materials. The loss factors of the polyurethanes were somewhat higher than desirable for our application. Furthermore, the range of dielectric properties realized by the addition of titanium dioxide was minimal. The loss factors of the polyethylene and polystyrene samples were below the sensitivity of our measurements. The real part of the permittivity for polyethylene was consistent with published handbook values. The polystyrene-titanium dioxide result was somewhat lower than specified by the manufacturer. Polystyrenes or resins with similar loss properties, loaded with titanium dioxide, remain candidates for use in constructing graded-layer dielectric bends.

Contents

1. Introduction

We have been exploring approaches to the approximate realization of graded dielectric transmission line bends for low-dispersion propagation of ultra-wideband pulses. In our initial experiment, we built a graded strip line bend with machined layers of dielectric materials, which included ultra-high-molecular-weight (UHMW) polyethylene and polystyrene loaded with varying quantities of titanium dioxide (TiO_2) ([1] and [2 (Appendix A)]). In search of an approach that would permit direct casting (rather than machining and assembly) of layered bends, we identified a two-part urethane casting resin as a base material to which varying quantities of titanium dioxide or other fillers might be added to adjust the dielectric properties.

In this note we describe time domain measurements of the complex permittivity, both of cast samples of several polyurethane formulations, as well as machined samples of the polyethylene and polystyrene used previously. Although the measurement methodology has been previously described in [3] and [4], here we employ a different test fixture. We summarize the methodology here and refer the reader to [3] for the details of the measurement and analysis procedures. As a subjective check on the quality of the permittivity data extracted from our measurements, we compared the observed transmission of an impulse through each sample with the prediction calculated on the basis of that permittivity data.

In contrast to the coaxial test fixture used in the earlier work, which had a circular cross section and a 100 cm long sample chamber, the fixture built for this effort had a rectangular cross section with a strip center conductor and a 20 cm sample chamber. The new test fixture design was intended to minimize the occurrence of air gaps at the center conductor and to reduce the significance of those that might occur. The fit between the samples and the center conductor can be extremely tight with this design, since a "slip-fit" over the center conductor is not required. Also, since most of the center conductor surface is flat, field enhancement is reduced, minimizing the impact of air gaps along those surfaces.

We begin now by summarizing the theory used to extract the complex permittivity from impulse transmission data. This is followed by a description of the experimental apparatus. We conclude by presenting the sample data for the various resin samples.

2. Theory

2.1 Complex Permittivity Calculation

As described in [3], our time domain measurement technique is based on separate impulse transmission measurements through two lengths of dielectric material, with unknown relative permittivity, ε_r, in an air-filled coaxial transmission line test fixture. For one measurement, the sample length is ℓ_1; for the other, it is increased to ℓ_2. In both cases, an identical impulse is launched from one side of the fixture and the transmitted pulse is recorded on the other side. The relative transmission measurement, which is the signal transmitted through the long sample normalized to the signal transmitted through the short sample, is

$$\begin{aligned} T_r(\omega) &= e^{-jk_o(\ell_2-\ell_1)\left(\sqrt{\varepsilon_r}-1\right)} \\ k_o &= \omega/c \end{aligned} \tag{1}$$

where an $e^{j\omega t}$ time dependence is assumed and c is the free space speed of light. This expression is also recognized as the impulse response for a length of material ℓ_2–ℓ_1, relative to the same length of air. Thus, $T_r(\omega)$, can be obtained as the frequency domain ratio of the two time domain measurements. Since Fresnel losses at the dielectric-air interfaces are identical for the two measurements, they cancel each other and need not be accounted for explicitly.

The above expression can be inverted to obtain the complex permittivity in terms of the natural logarithm of $T_r(\omega)$. After unwrapping the phase and solving for ε_r, we obtain

$$\varepsilon_r(\omega) = \left[\frac{j \ln\left[T_r(\omega) e^{j\omega\tau_o}\right] + \omega\tau_o}{k_o(\ell_2-\ell_1)} + 1 \right]^2 \tag{2}$$

where τ_o is the delay to the peak in the time domain impulse response and the argument of the logarithm is the phase-unwrapped frequency domain response. Note that with the time convention used here, a positive imaginary part of the permittivity is non-physical.

2.2 Loss Tangent and Attenuation Coefficient Calculations

The attenuation of a dielectric material is often expressed in terms of its loss tangent. The loss tangent is defined by

$$\tan[\delta] = -\mathrm{Im}[\varepsilon_r]/\mathrm{Re}[\varepsilon_r] \tag{3}$$

where the complex permittivity is expressed in terms of real and imaginary parts as

$$\varepsilon_r = \mathrm{Re}[\varepsilon_r](1 - j\tan[\delta]) \tag{4}$$

In [3] it is shown that the attenuation in decibels per unit length *within* a dielectric material can be calculated from

$$\alpha|_{dB/cm} = 0.08686\, k_o\, n''(\omega) \tag{5}$$

where k_o is expressed in rad/m, $n''(\omega) = -\mathrm{Im}[n(\omega)]$, and $n(\omega) = n'(\omega) - jn''(\omega) = \sqrt{\varepsilon_r(\omega)}$, is the complex index of refraction, with n' and n'' positive and real.

2.3 Validation of the Complex Permittivity Measurement

Once we have calculated a complex permittivity using the methods of the previous section, we require a method of confirming our calculation. To do so, we predict the transmitted waveform through a dielectric slab, given the waveform transmitted through an air-filled line.

In order to predict the voltage transmitted through a dielectric slab, we first use the measured complex permittivity to calculate the transmission coefficients at the front and back interfaces. These are

$$\tau_1(\omega) = \frac{2}{\sqrt{\varepsilon_r(\omega)} + 1}, \qquad \tau_2(\omega) = \frac{2\sqrt{\varepsilon_r(\omega)}}{\sqrt{\varepsilon_r(\omega)} + 1} \tag{6}$$

Then, we calculate the propagation factor through the slab, relative to the same length of air, as

$$T(\omega) = e^{-j\,k_o\left(\sqrt{\varepsilon_r(\omega)} - 1\right)\ell} \tag{7}$$

where k_o is the free-space propagation coefficient and ℓ is the sample length. By calculating relative to air, we introduce a time correction to compensate for the reduction in the air path length that occurs as dielectric material is added to the test fixture. Now, the frequency domain transmitted voltage is

$$V(\omega) = \tau_1(\omega)\ \tau_2(\omega)\ T(\omega)\ V_{air}(\omega) \tag{8}$$

By transforming this transmitted voltage to the time domain, we obtain the desired result for comparison with the observed waveform measurement.

3. Experimental Measurement Technique

The time domain measurement technique used the transmission of plane wave impulses through a rectangular "coaxial" transmission line test fixture containing uniform samples of polymeric resin dielectrics. Photos of the test fixture and a diagram of the fixture and the measurement setup are shown below.

Top view of open test fixture:

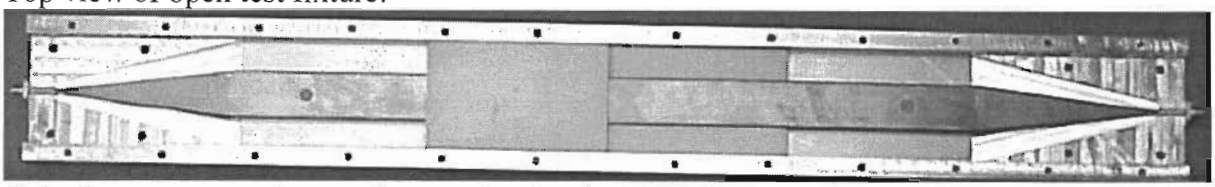

Only the access panels over the sample chamber must be opened to insert or remove samples. Here, three of four sample sections are installed. The upper portions of the tapered sections and all four upper access panels have been removed.

Input/output connector interface detail:

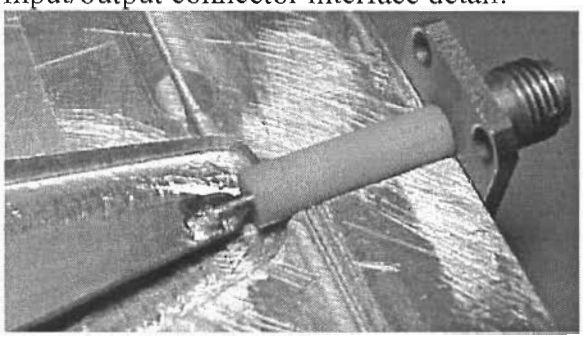

Sample chamber detail:

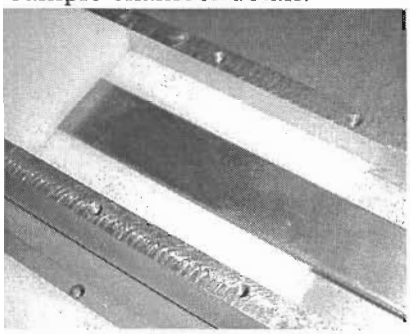

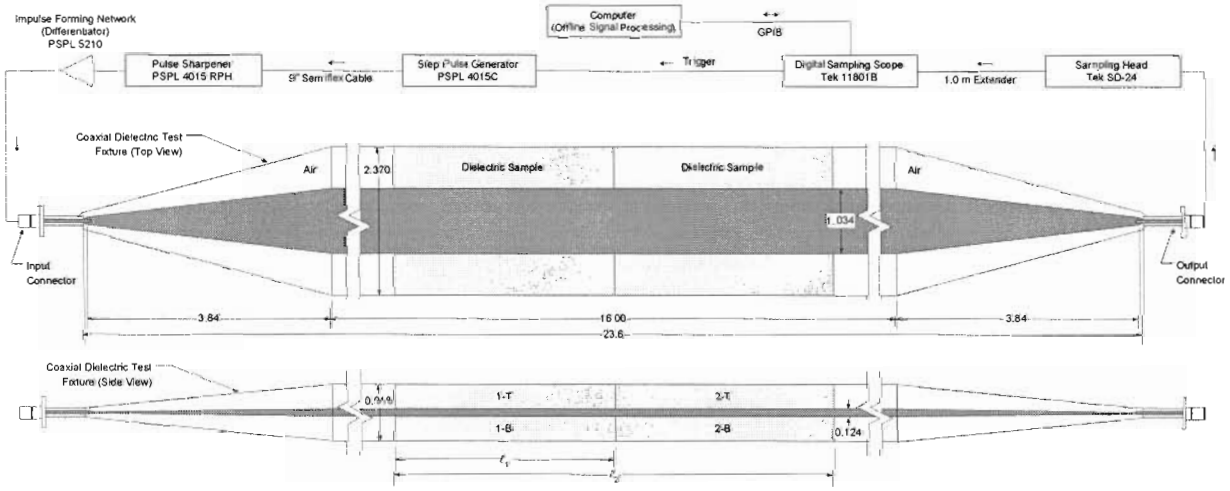

Figure 1. Test fixture and block diagram of instrumentation setup for complex permittivity measurements. Fixture dimensions are in inches.

A design goal for the test fixture was a 50 Ω impedance throughout; and the input and output taper sections were designed to introduce, at most, 15 ps of dispersion. Finite element analyses similar to those described in [2] were used to adjust the cross section dimensions of the sample chamber (see Figure 3) to produce an impedance of 50 Ω. The TDR in the following figure shows that the sample chamber approached the 50 Ω design goal, while there was significant deviation from that goal within the tapered regions. The figure indicates the sources within the test fixture of the various TDR features. The high impedance spikes correspond to the emergence of the connector center conductors from their Teflon dielectric sheaths. The impedance then decreases gradually through the tapered sections. The impedance "dips" on either side of the sample region correspond to the nylon posts that support the center conductor.

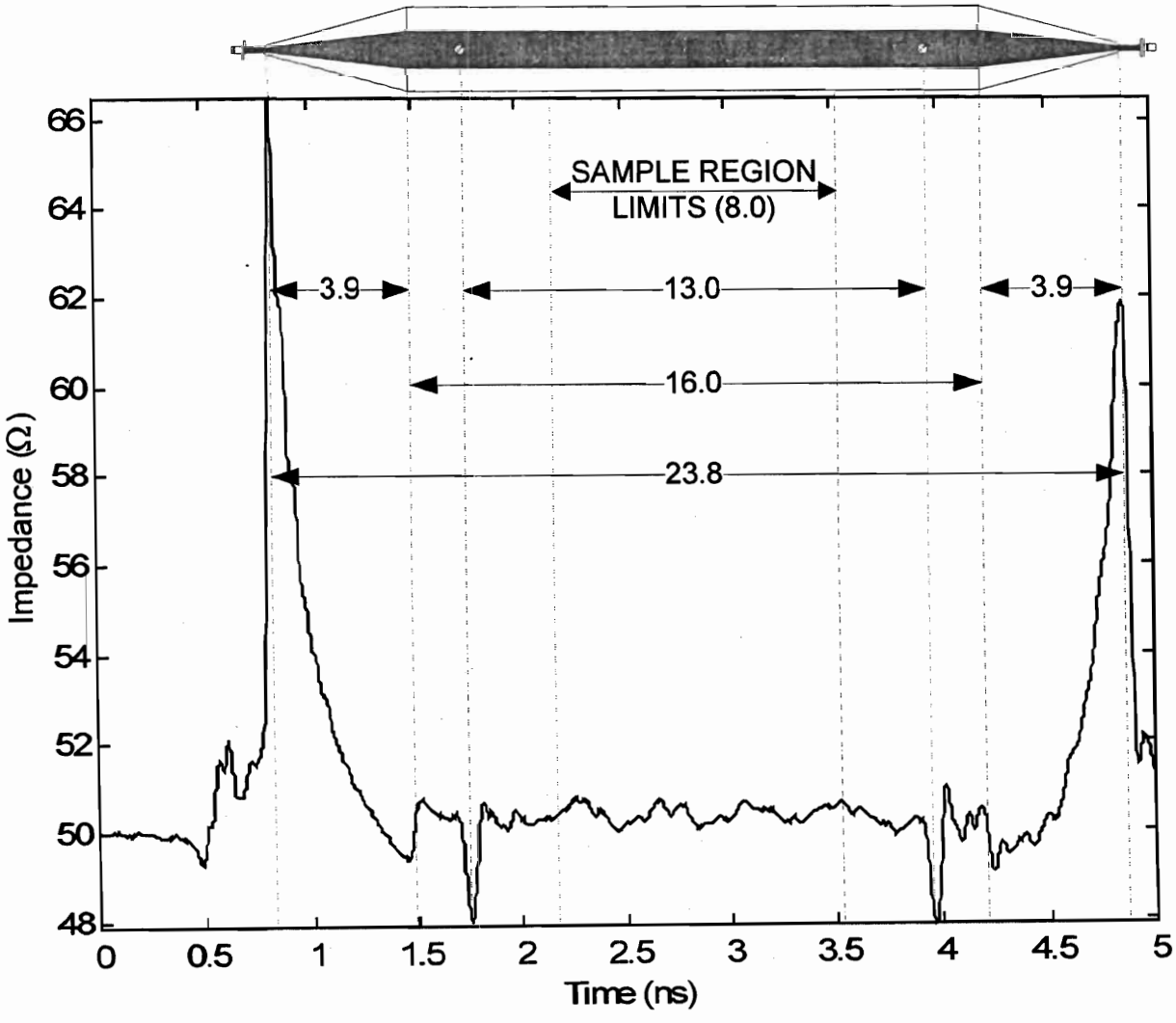

Figure 2. TDR impedance map of the test fixture. The TDR is correlated with the test fixture geometry. Significant test fixture dimensions (in inches) are annotated.

The polymeric resin samples were cast in aluminum molds or machined from pre-cast slabs of material. Each sample set consisted of two pairs of top and bottom sample halves. The four pieces are identified in the diagram in Figure 1 as the pairs 1-T, 1-B, and 2-T, 2-B. The number "1" pair formed a short sample; the combination of number "1" and number "2" pairs formed a long sample. Sample lengths were precisely measured with a digital caliper. The cross section of each top-bottom pair matched the cross section of the sample chamber as shown in the following figure. Access to the sample chamber of the test fixture for installation and removal of samples was by way of upper and lower access panels.

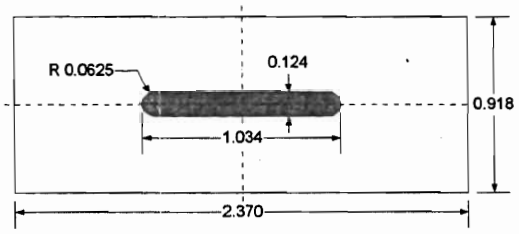

Figure 3. Test fixture cross section. The outer walls are aluminum; the center conductor strip is copper. The impedance of this structure, when filled with air, is 50 Ω. Dimensions are in inches.

The pulse transmitted through the test fixture is modified by a characteristic time delay, attenuation, and dispersion. By comparing the transmitted waveforms for two different sample lengths, as described previously, we determine the propagation properties for a length of dielectric equal to the difference between the two sample lengths. This differential measurement eliminates system instrumentation response effects and the effects of Fresnel losses at entry and exit dielectric-air interfaces.

4. Dielectric Material Measurements

We measured the complex permittivity of three different polymeric resins, UHMW polyethylene, polystyrene loaded with TiO_2 , and several polyurethane-based formulations. The polystyrene was an adjusted dielectric product known as Eccostock HiK®, produced by Emerson & Cuming Microwave Products. The manufacturer quoted its relative dielectric constant as 4.4. The polyurethane formulations were all based on R1 Fast Cast® No. 709 two-part urethane resin, by Goldenwest Manufacturing, Inc. Six formula variations were measured: (1) plain R1 resin with no fillers or additives, (2) R1 with 50% by volume of butterboard (BB) filler added, (3) R1 with 50% by volume of solid glass microsphere (HG3000) filler added, (4) R1 with 5% by volume of TiO_2 pigment dispersed in ethylene glycol, $Et(OH)_2$, (5) R1 with 25% by weight of TiO_2 powder added, and (6) R1 with 37% by weight of TiO_2 powder added. Below, we present the measurement results for each of these materials.

4.1 Air Reference

Air reference data were never used in calculation of complex permittivity results. They serve to indicate the magnitude of the system bandwidth and as the starting point for predictive calculations of impulse propagation based on the measured permittivity.

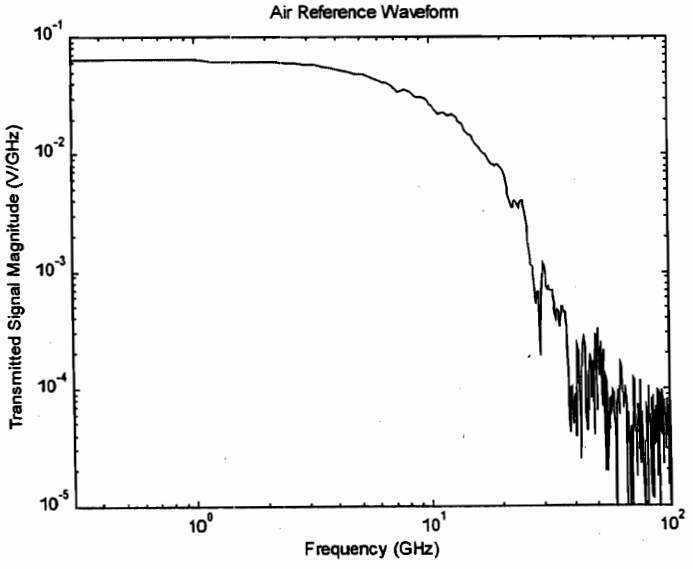

Figure 4. The air spectral response associated with UHMW polyethylene measurements. The indicated bandwidth is about 20 GHz. The corresponding time domain data are presented below.

4.2 UHMW Polyethylene

The polyethylene sample materials were machined to fit the test fixture from sheet stock. This material has a dielectric constant of 2.3 and a loss tangent below 0.0005. On the basis of signal transit time, we observed a dielectric constant of 2.3. The signal processing of the transmitted waveforms produced the same value for the real part of the complex permittivity over a range of 0.5 to 6 GHz. Since our loss tangent was negative at low frequencies, we conclude our measurement was not sufficiently sensitive to determine the loss. Measured and calculated impulse transmission data agree well with respect to transit time. The calculated peak heights are somewhat low, owing probably to an over-estimate of the high frequency loss.

Graphical representations of the sample measurement data follow. Note that the two transmitted waveforms (Figure 5) are nearly identical, making a precise measurement of the loss tangent very difficult. Note also that the processed data are probably not valid above 10 GHz or so, due to attenuation by the low-pass filter used in the signal processing algorithm.

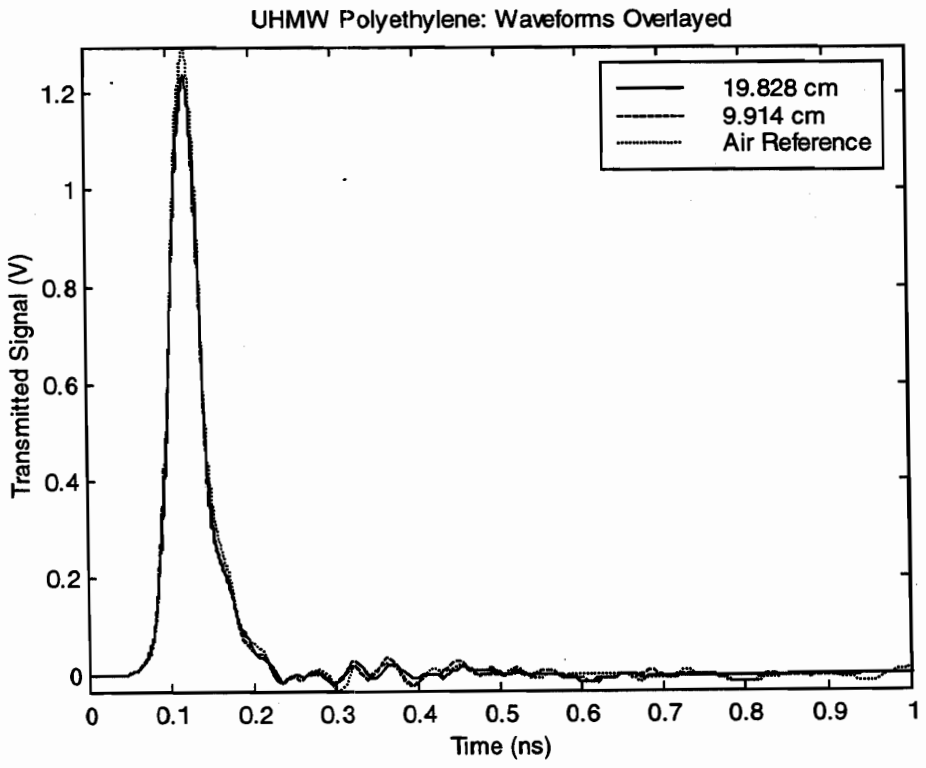

Figure 5. Overlay of waveforms transmitted through UHMW polyethylene with an air reference. For these peaks, the FWHM is in the range from 41 to 42 ps. The measurements were truncated beyond 0.23 ns for processing.

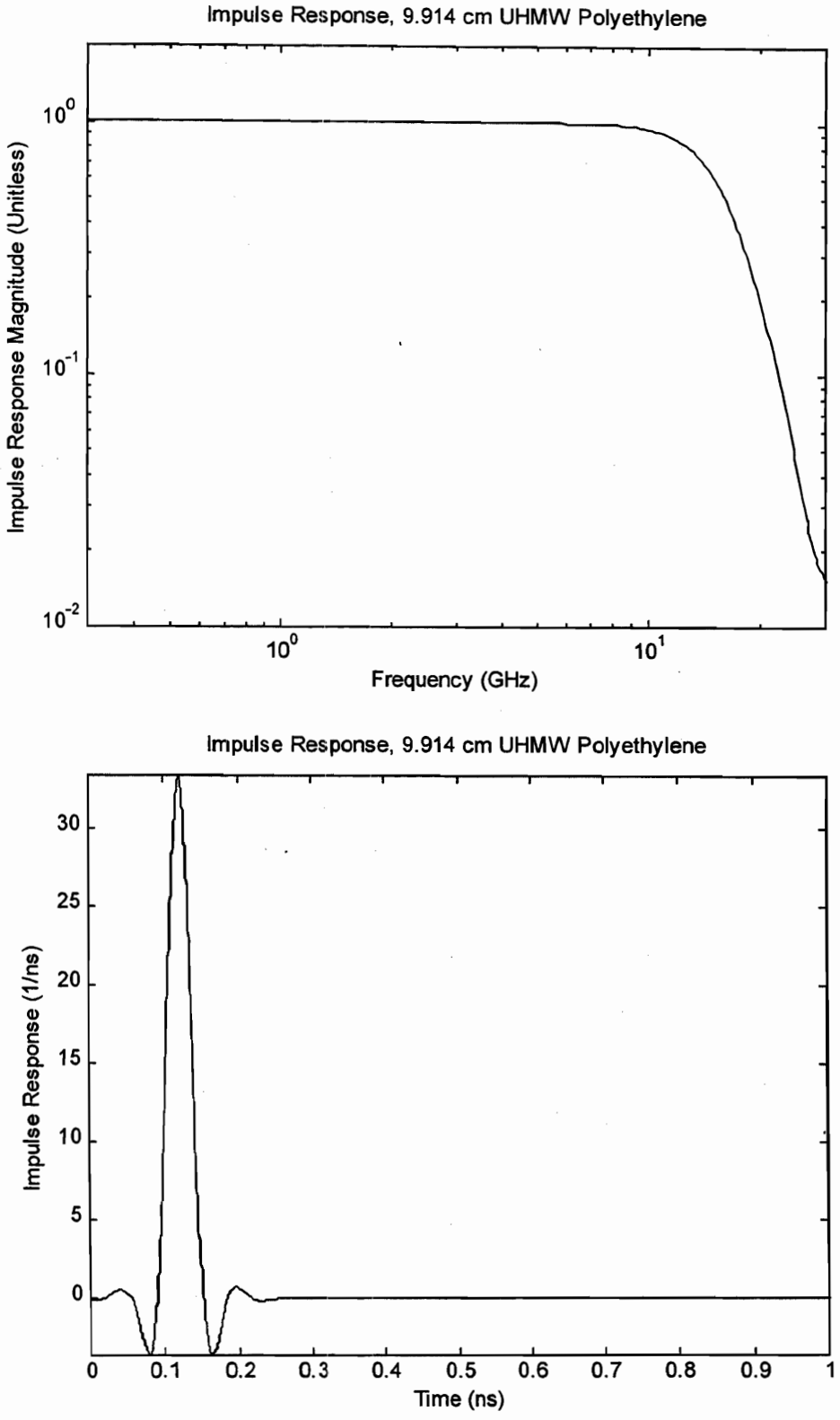

Figure 6. UHMW polyethylene impulse response. The signal processing employed a third order modified Butterworth filter at 16 GHz. The FWHM in the time domain is 34 ps.

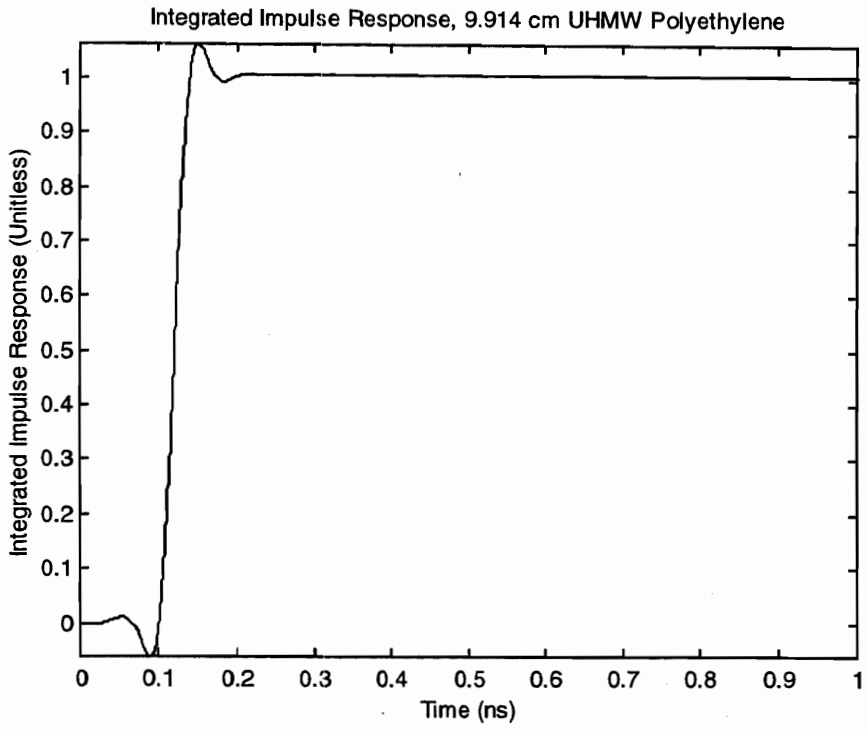

Figure 7. . Integral of UHMW polyethylene impulse response. The rise time is 30 ps.

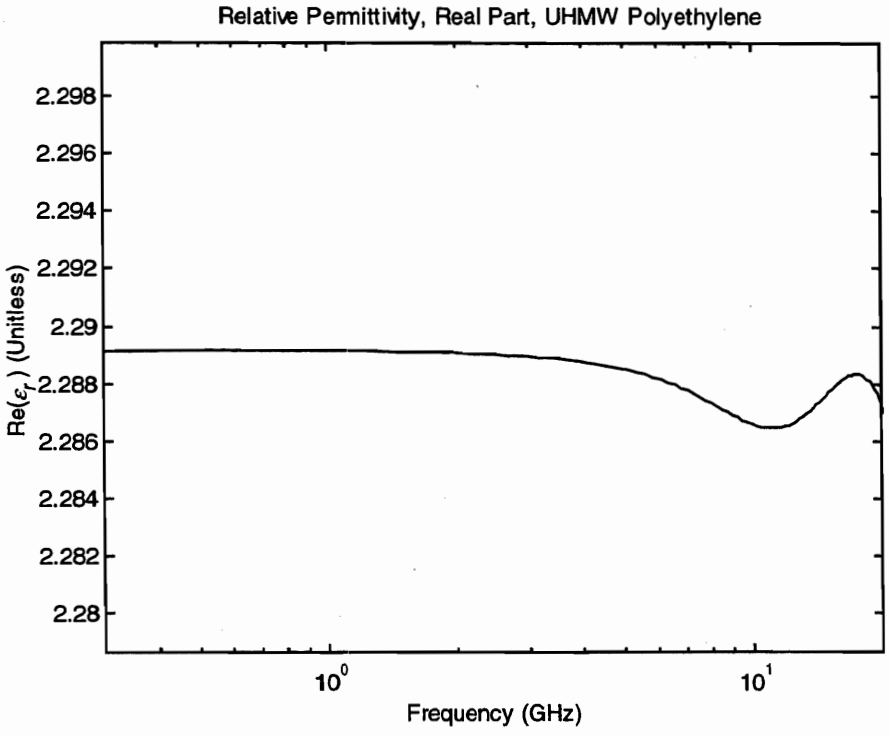

Figure 8. UHMW polyethylene real part of permittivity.

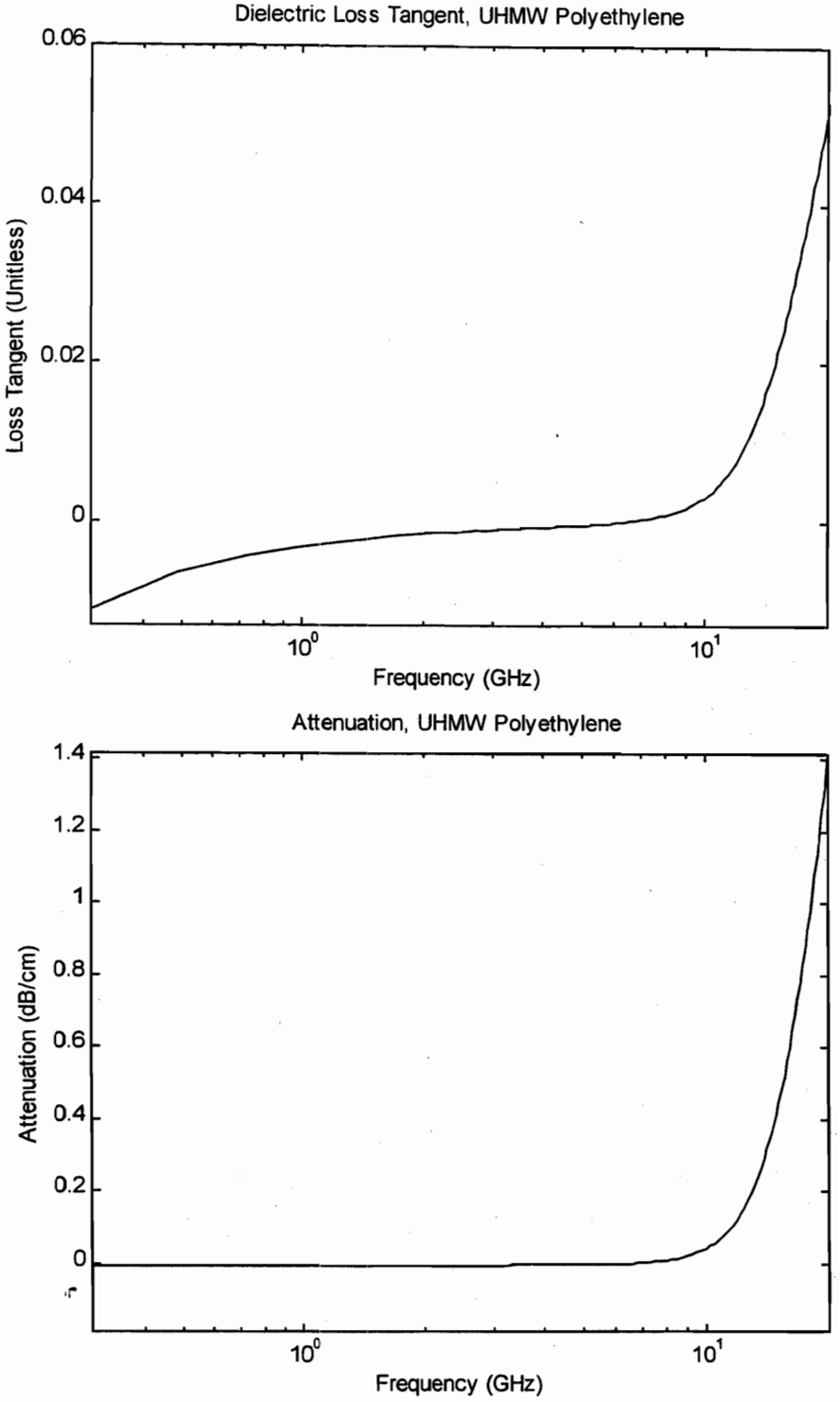

Figure 9. UHMW polyethylene loss tangent and attenuation. Since negative quantities are non-physical, their occurrence indicates a result very close to zero, with a small amount of noise.

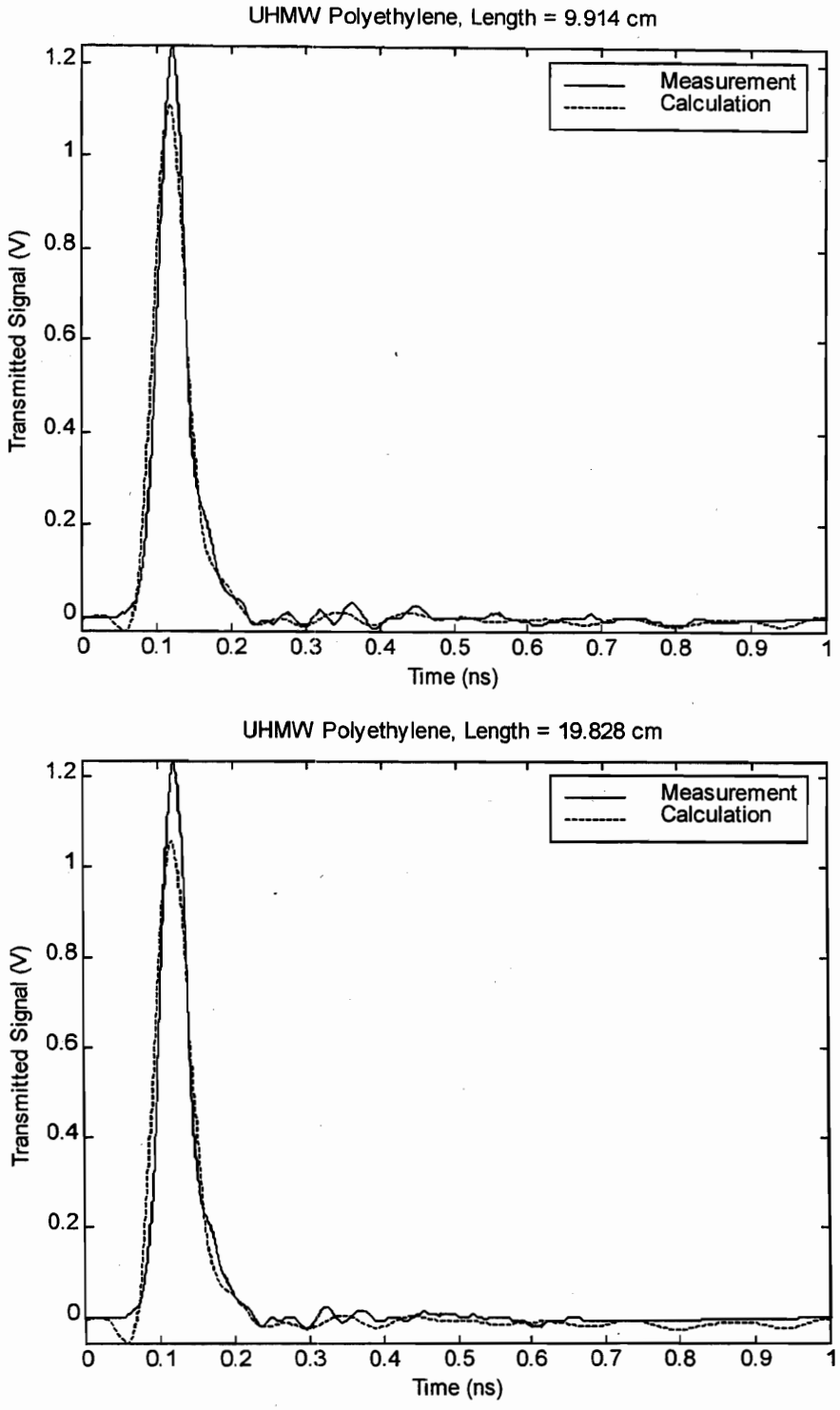

Figure 10. UHMW polyethylene transmitted waveforms, measured and calculated. Transit times agree to within 3 ps, although there is some extraneous loss in the calculated data.

4.3 Eccostock HiK (K≈4.4)

The polystyrene sample materials were machined to fit the test fixture from Emerson & Cuming sheet stock. The manufacturer specified the dielectric constant as 4.4±3% with a loss tangent below 0.002. On the basis of signal transit time, we observed a dielectric constant in a range of 4.0 to 4.3. The signal processing of the transmitted waveforms produced 4.0 for the average real part of the complex permittivity over a range of 0.5 to 16 GHz. The loss tangent was 0.013 over the same frequency range, about five times higher than the manufacturer's specification. There are small transit time differences between measured and calculated impulse transmission data. The calculated peaks arrive early, suggesting that the measured dielectric constant may be too small. The calculated peak heights are about 10% low, indicating a possible over-estimate of the loss.

Graphical representations of the sample measurement data follow. Note that the processed data are probably not valid above 10 GHz or so, due to attenuation by the low-pass filter used in the signal processing algorithm.

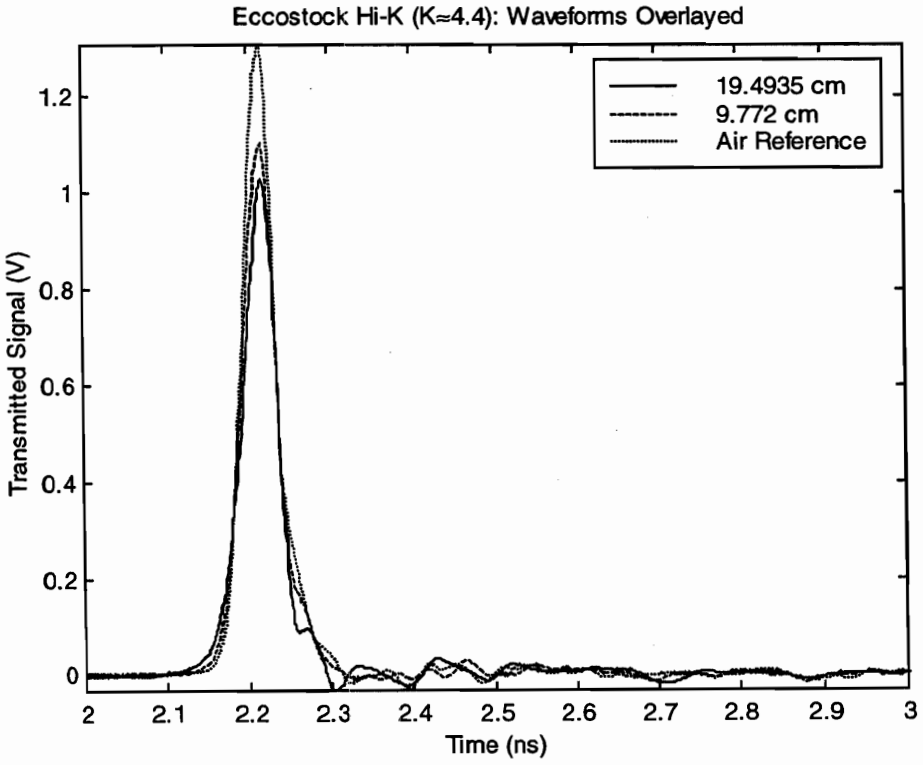

Figure 11. Overlay of waveforms transmitted through Eccostock HiK polystyrene with an air reference. For the sample peaks, the FWHM is 47 ps. The measurements were truncated beyond 2.3 ns for processing.

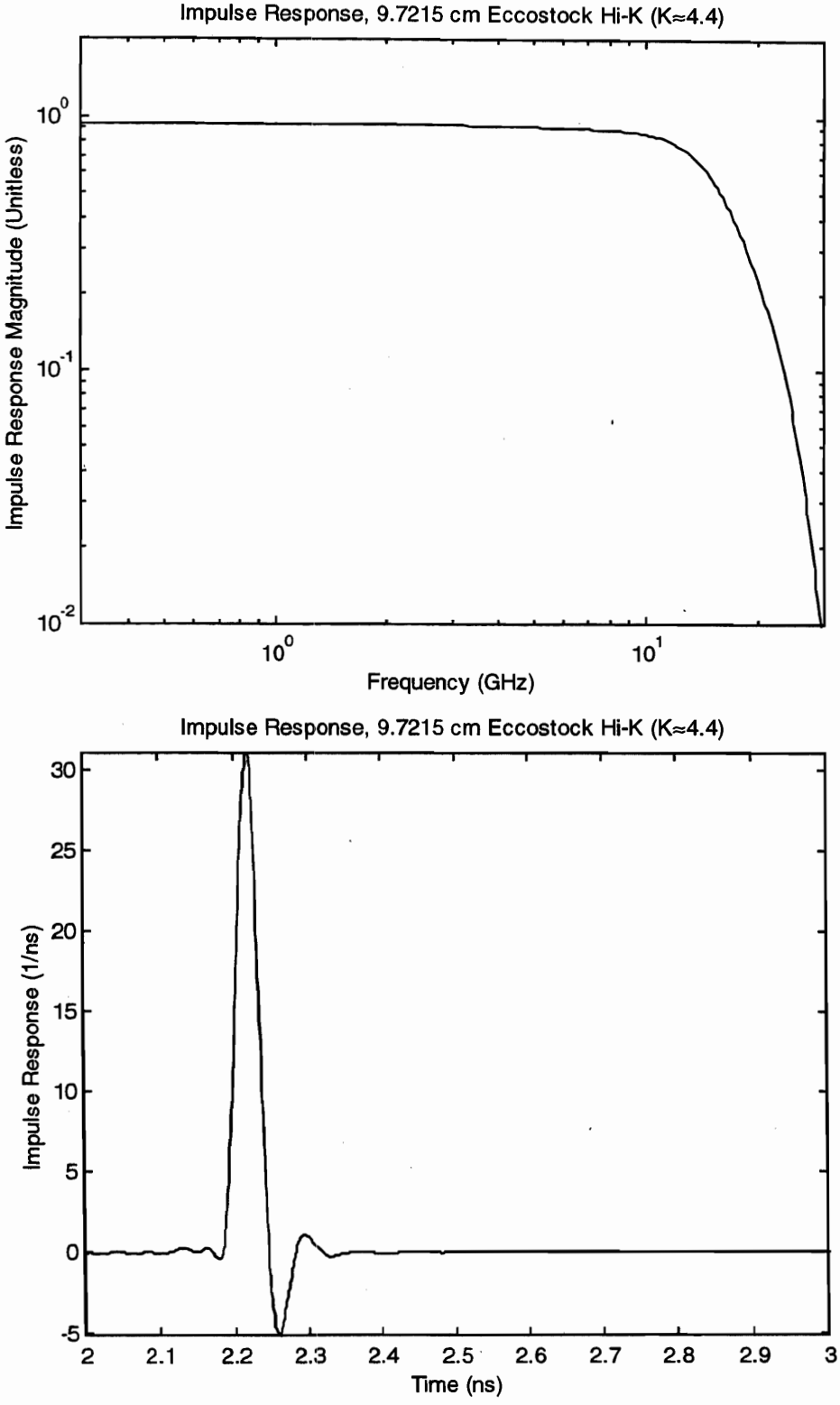

Figure 12. Eccostock HiK impulse response. The signal processing employed a third order modified Butterworth filter at 16 GHz. The FWHM in the time domain is 33 ps.

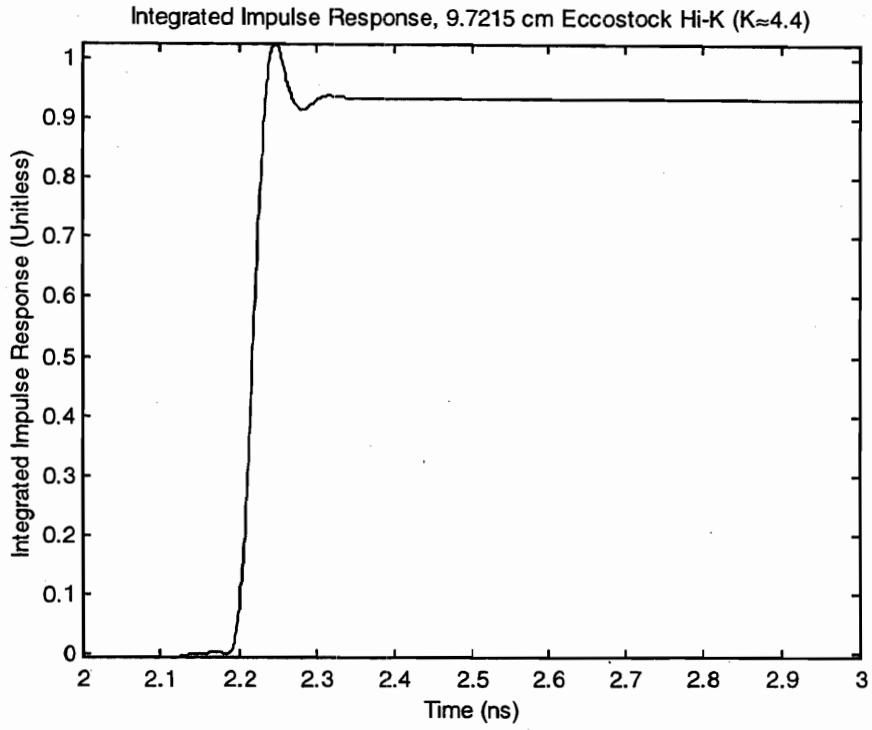

Figure 13. Integral of Eccostock HiK impulse response. The rise time is 32 ps.

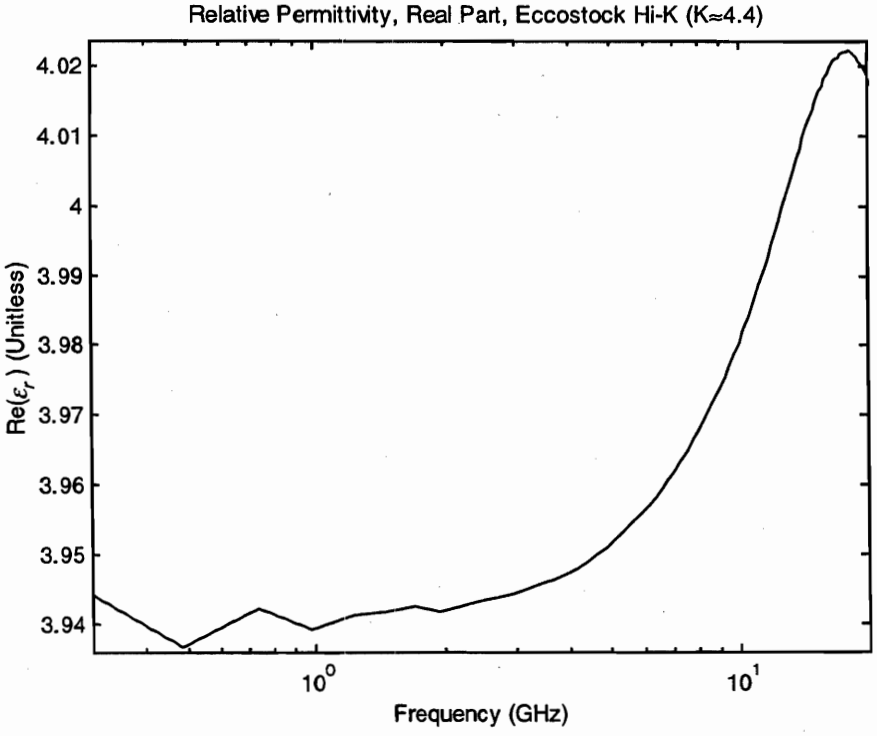

Figure 14. Eccostock HiK real part of permittivity.

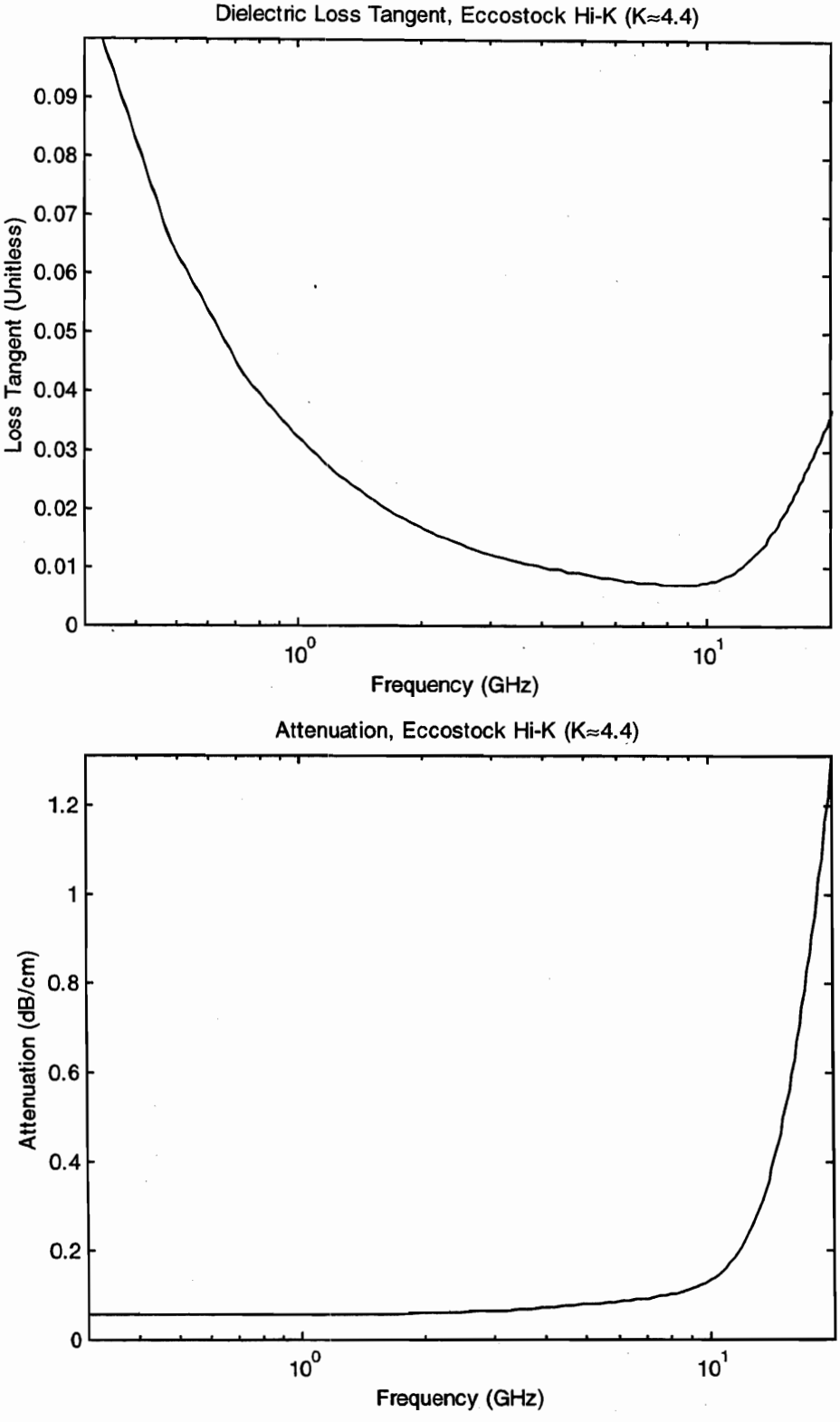

Figure 15. Eccostock HiK loss tangent and attenuation.

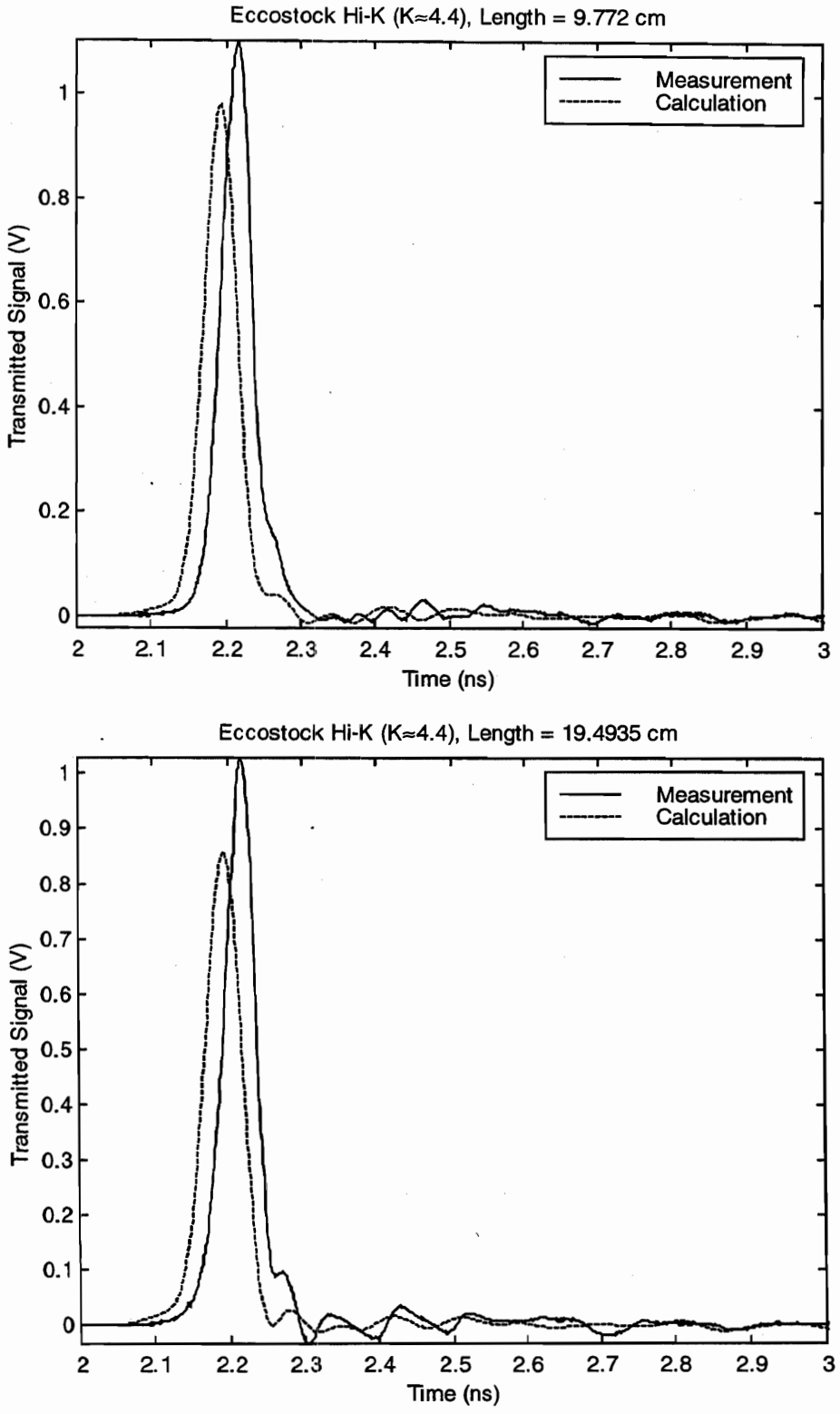

Figure 16. Eccostock HiK transmitted waveforms, measured and calculated. Calculated transit times are short by about 22 ps, and the calculated peak heights are somewhat low.

4.4 R1 Fast Cast 709 Polyurethane

The polyurethane sample materials were prepared by casting the two-part R1 Fast Cast resin mixtures in a set of four identical aluminum molds. Pure "A" and "B" parts have a viscosity slightly greater than water. Equal volumes of each are blended at room temperature and poured into the molds. Setting time is only seven minutes, and castings can be de-molded within a half hour. Complete curing occurs over night. After curing, sample pair was trimmed to uniform length. Generally, each sample pair was trimmed to approximately the same length; so that our short measurement samples were usually about half the length of the long samples.

When butterboard (BB) or solid glass micro-sphere (HG3000) fillers were added, they were blended at a rate of 50% by volume with each of the separate "A" and "B" parts. Then the filled "A" and "B" parts were mixed and poured into the molds. Formulations employing TiO_2 powder filler were prepared in the same manner, except that the fraction of powder added was measured by weight rather than by volume. Sample sets with 25% and 37%[†] by weight of TiO_2 powder were prepared in this way. Following the supplier's instructions, the TiO_2 pigment dispersion was blended with the "B" part only, at a rate of 10% by volume. The resulting final castings had approximately 5% by volume of added dispersion, the maximum recommended percentage.

In the following, we present graphical representations of the sample measurement data for each of the five polyurethane sample sets. Note that the processed data are probably not valid above 10 GHz or so, due to attenuation by the low-pass filter used in the signal processing algorithm.

4.4.1. R1 Fast Cast (No additives, no fillers)

On the basis of signal transit time, we observed a dielectric constant in a range of 2.8 to 2.9. The signal processing of the transmitted waveforms produced 2.9 for the average real part of the complex permittivity over a range of 1 to 6 GHz. The loss tangent was 0.061 over the same frequency range. There are small transit time differences between measured and calculated impulse transmission data; the calculated peaks arrive about 25 ps late. Also, the calculated peak heights are somewhat low, indicating a possible over-estimate of the loss.

[†] This was the highest practical concentration of titanium dioxide. Part "A" and "B" mixtures were so viscous as to be barely pourable. The final mixture had to be poured into the molds with utmost care to avoid entrapment of air.

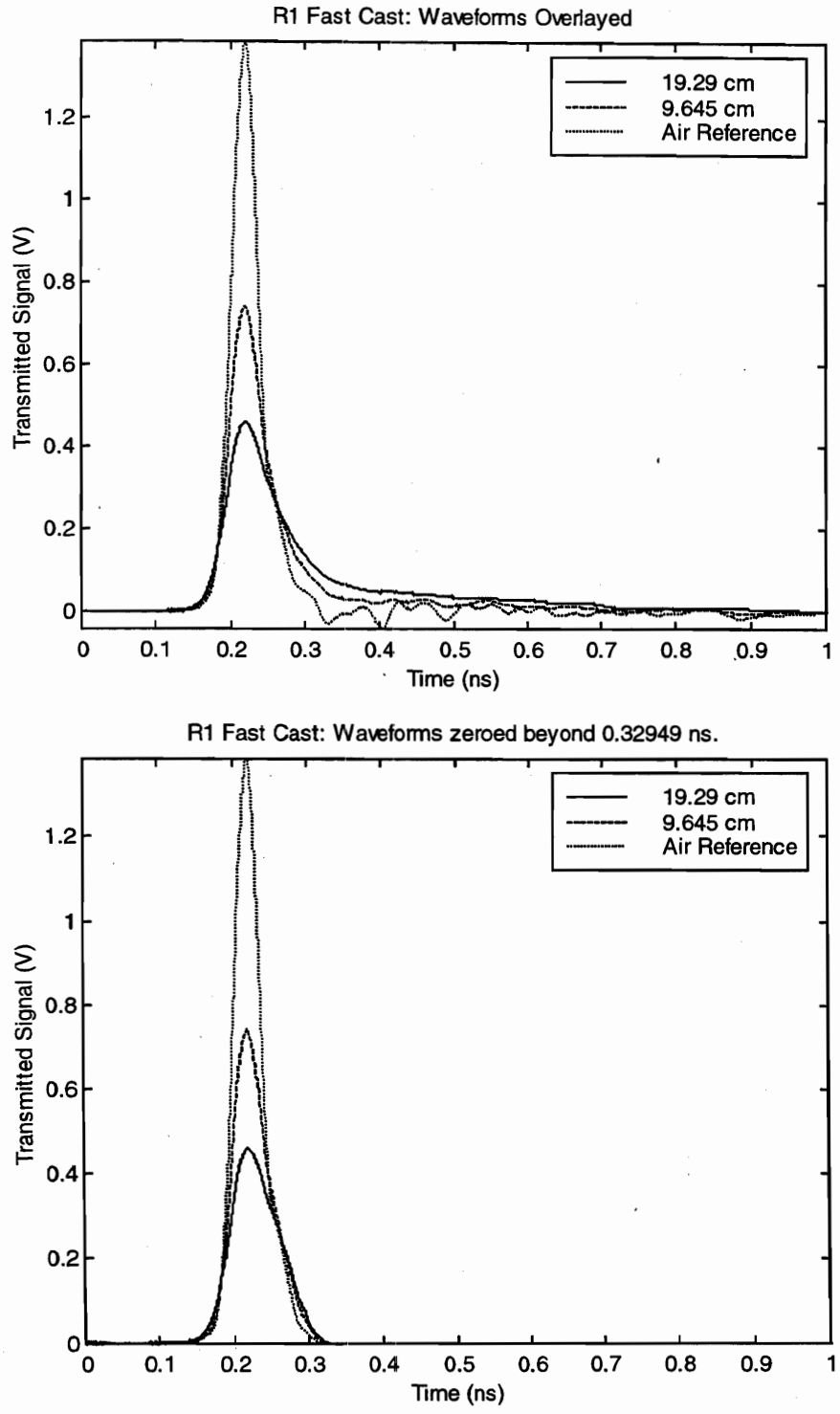

Figure 17. Overlay of waveforms transmitted through R1 Fast Cast with an air reference. For the short sample, the FWHM is 55 ps; for the long sample, we observe 78 ps. The measurements were truncated beyond 0.33 ns for processing. Without this arguably excessive truncation of the waveforms, the permittivity results exhibit unrealistic undulatory frequency dependence.

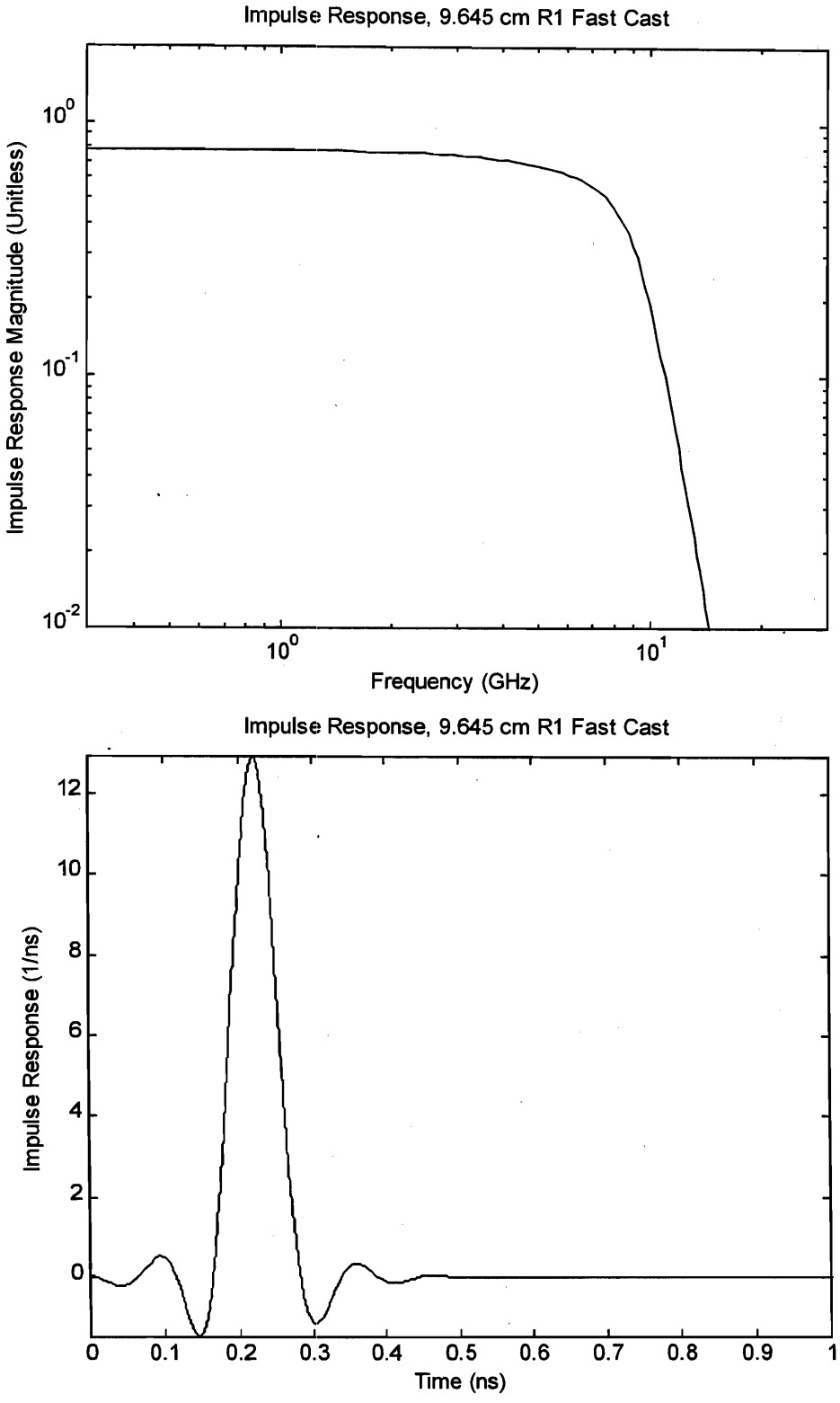

Figure 18. R1 Fast Cast impulse response. The signal processing employed a fifth order modified Butterworth filter at 10 GHz. The FWHM in the time domain is 65 ps.

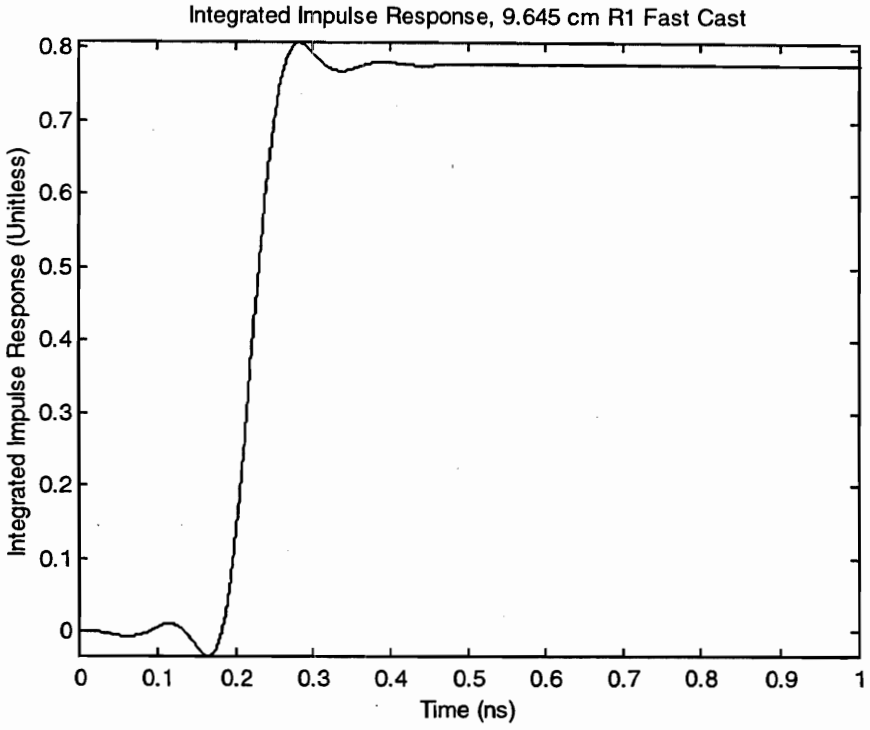

Figure 19. Integral of R1 Fast Cast impulse response. The rise time is 59 ps.

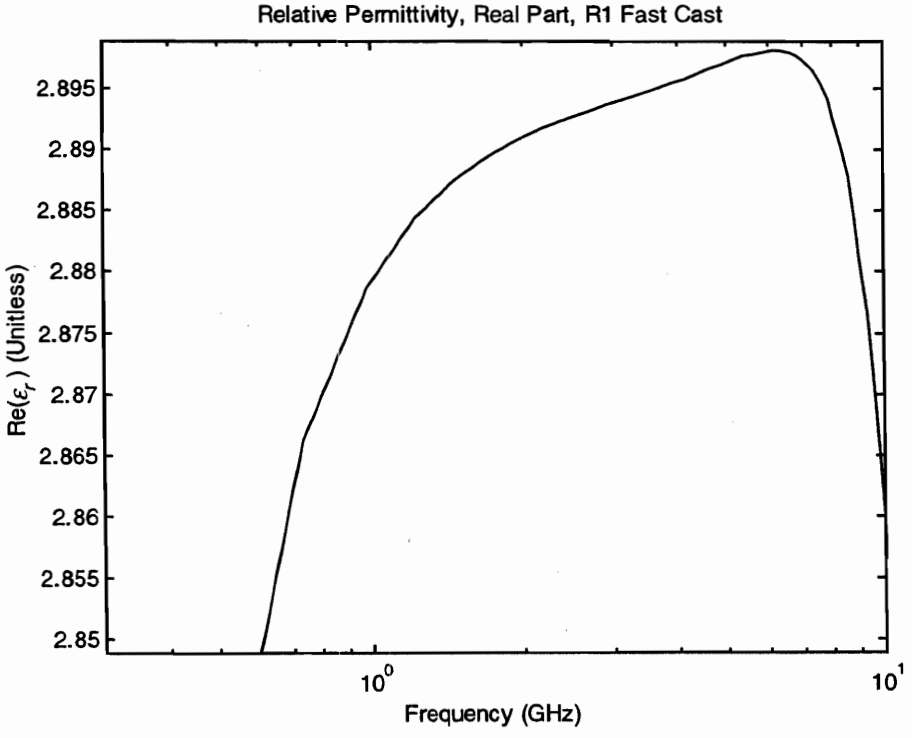

Figure 20. R1 Fast Cast real part of permittivity.

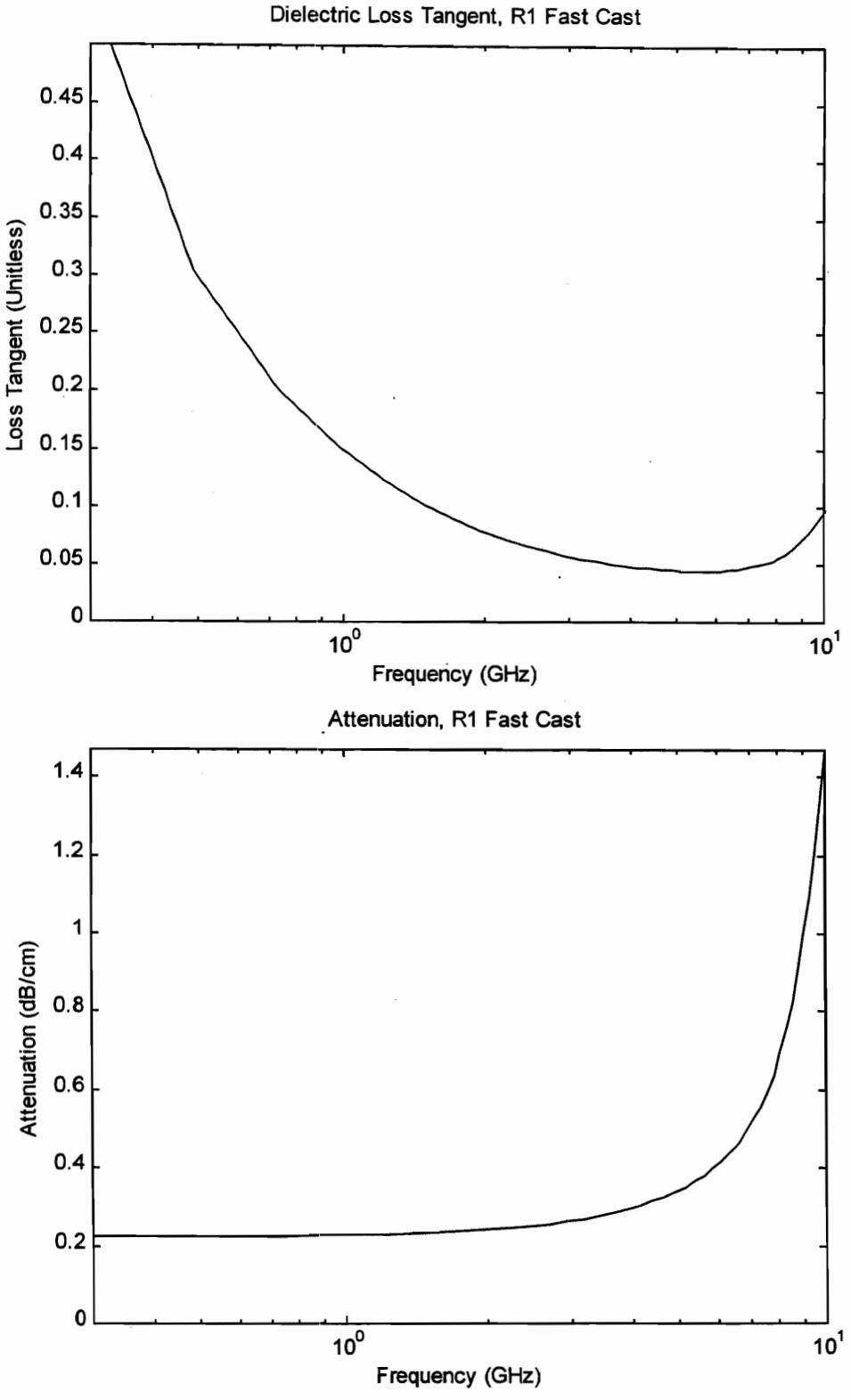

Figure 21. R1 Fast Cast loss tangent and attenuation.

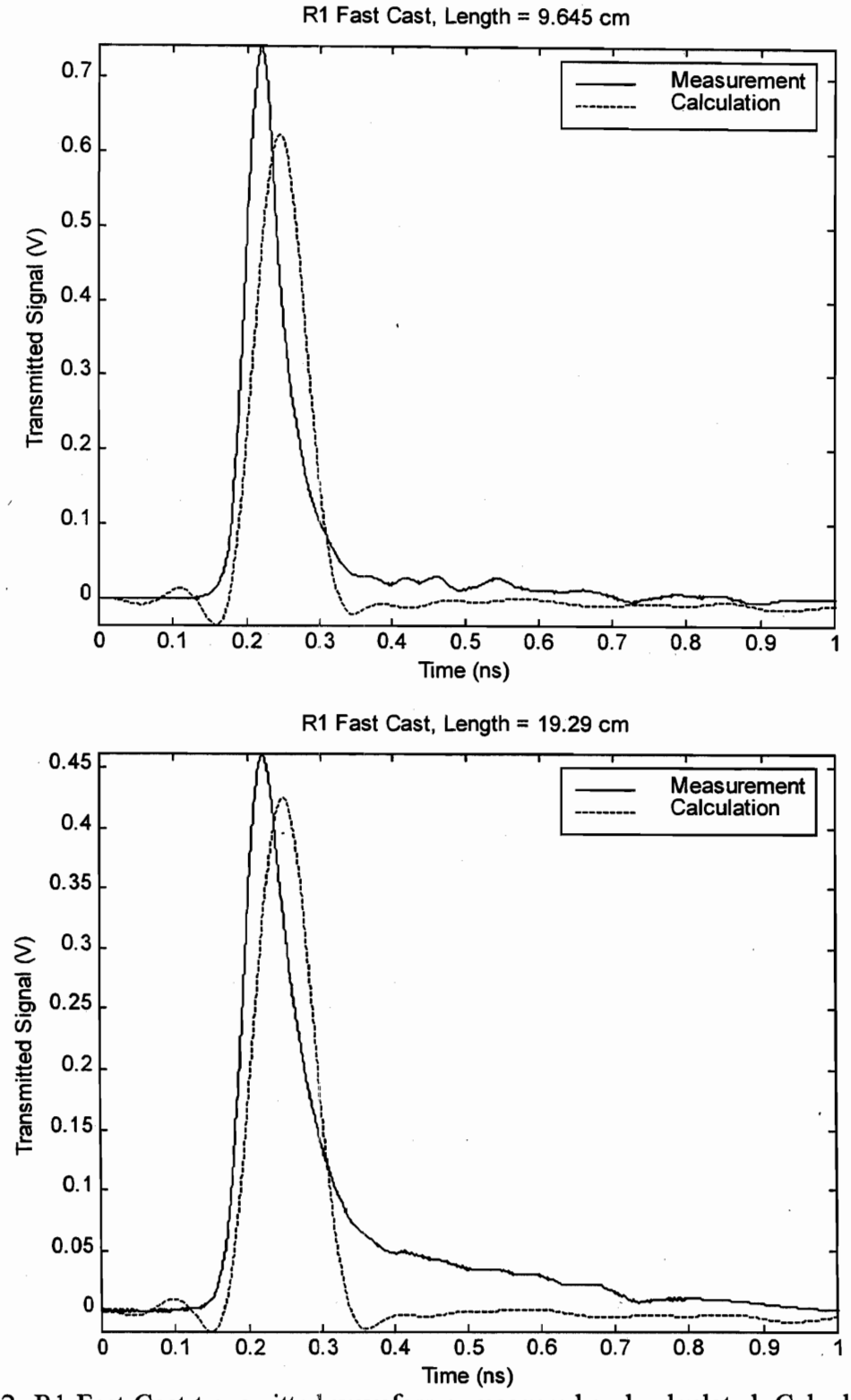

Figure 22. R1 Fast Cast transmitted waveforms, measured and calculated. Calculated transit times are long by about 25 ps, and the peak heights are somewhat low. As a result of the waveform truncation for processing, the late-time tails are not reproduced.

4.4.2. R1 Fast Cast, 50% Butterboard (BB) Filler

On the basis of signal transit time, we observed a dielectric constant of 2.1. The signal processing of the transmitted waveforms produced 2.1 for the average real part of the complex permittivity over a range of 1 to 6 GHz. The loss tangent was 0.054 over the same frequency range. Transit times for measured and calculated impulse transmission data are essentially identical. The calculated peak heights are somewhat low, indicating a possible over-estimate of the loss.

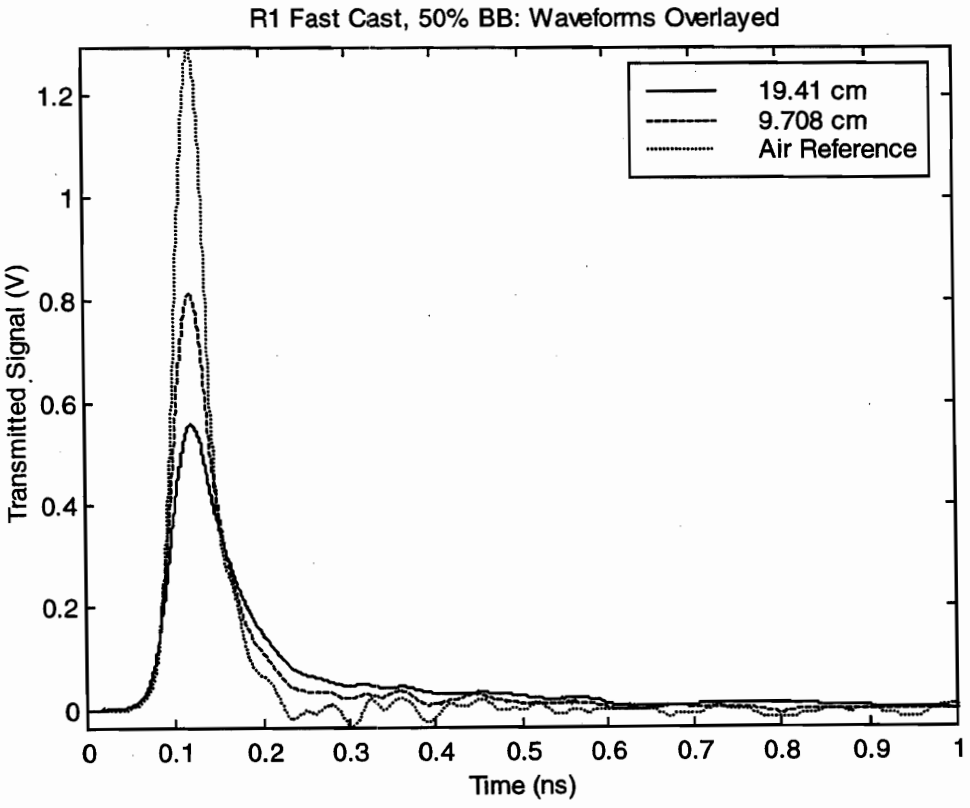

Figure 23. Overlay of waveforms transmitted through R1 Fast Cast containing 50% BB filler with an air reference. For the short sample, the FWHM is 52 ps; for the long sample, we observe 71 ps. The measurements were truncated beyond 0.23 ns for processing. Without this arguably excessive truncation of the waveforms, the permittivity results exhibit unrealistic undulatory frequency dependence.

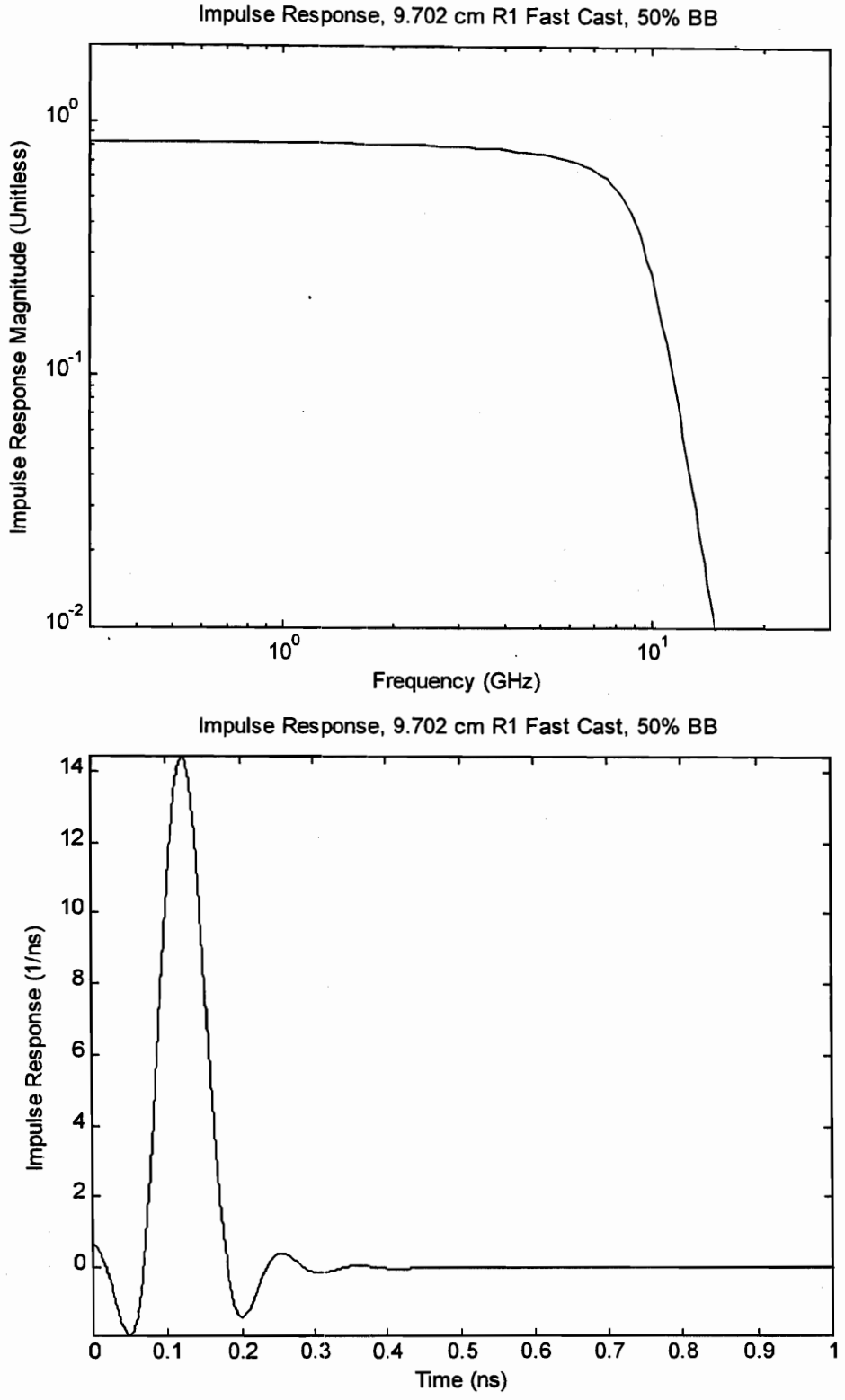

Figure 24. R1 Fast Cast with 50% BB filler, impulse response. The signal processing employed a fifth order modified Butterworth filter at 10 GHz. The FWHM in the time domain is 63 ps.

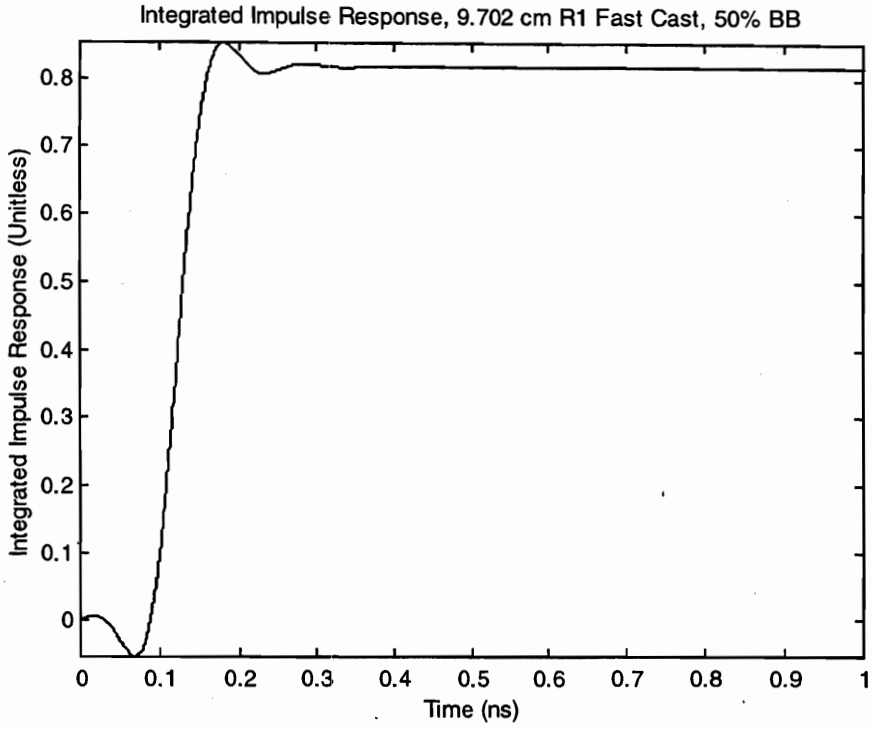

Figure 25. Integral of impulse response of R1 Fast Cast with 50% BB filler. The rise time is 56 ps.

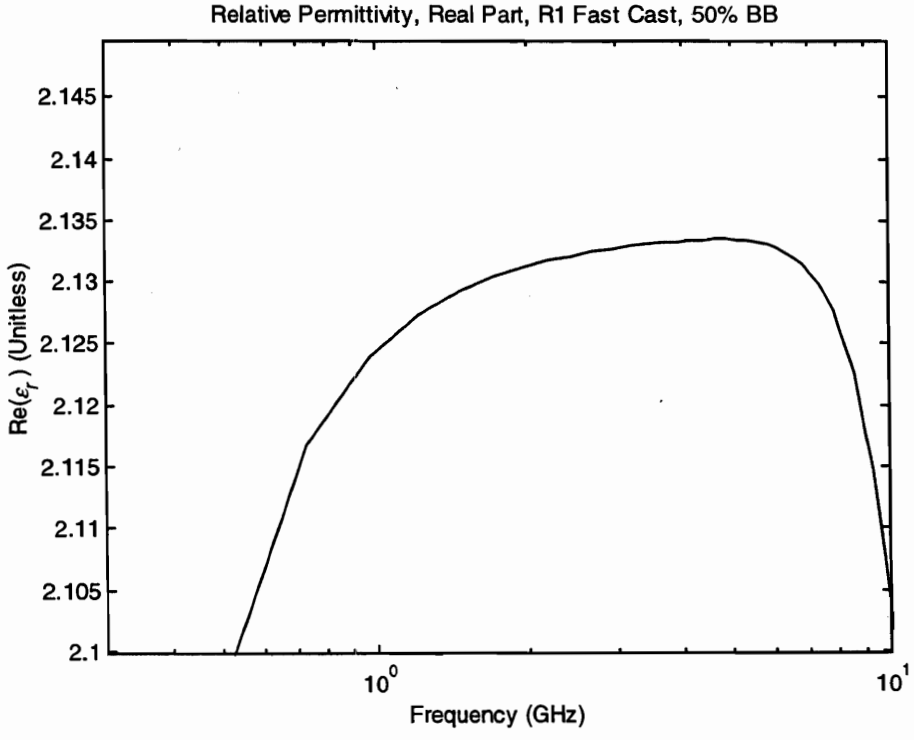

Figure 26. R1 Fast Cast with 50% BB filler, real part of permittivity.

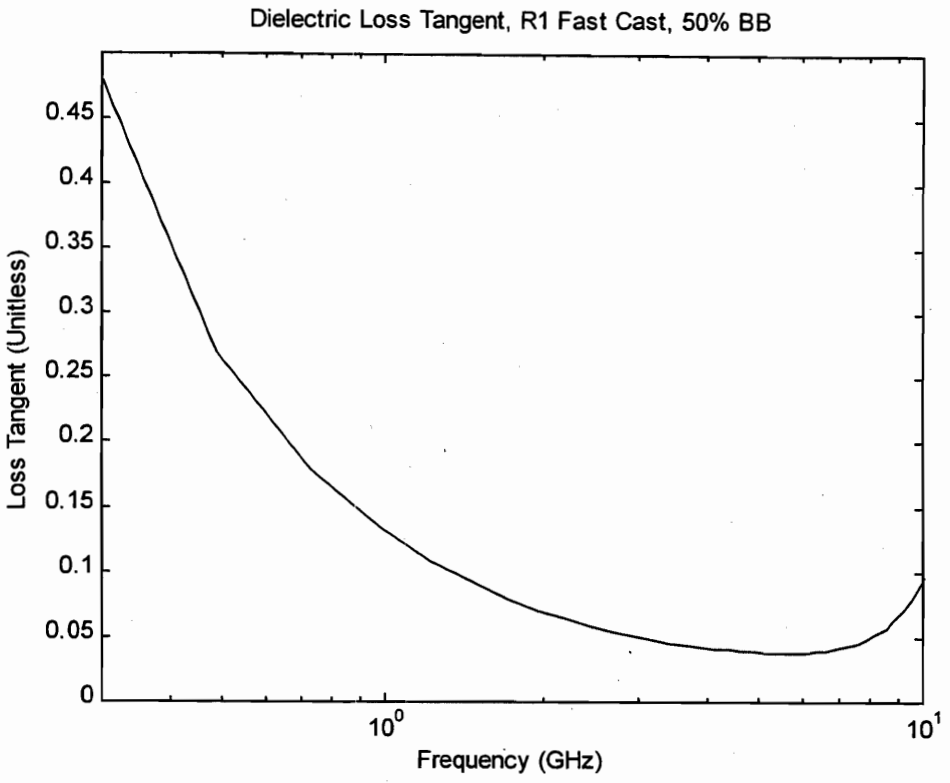

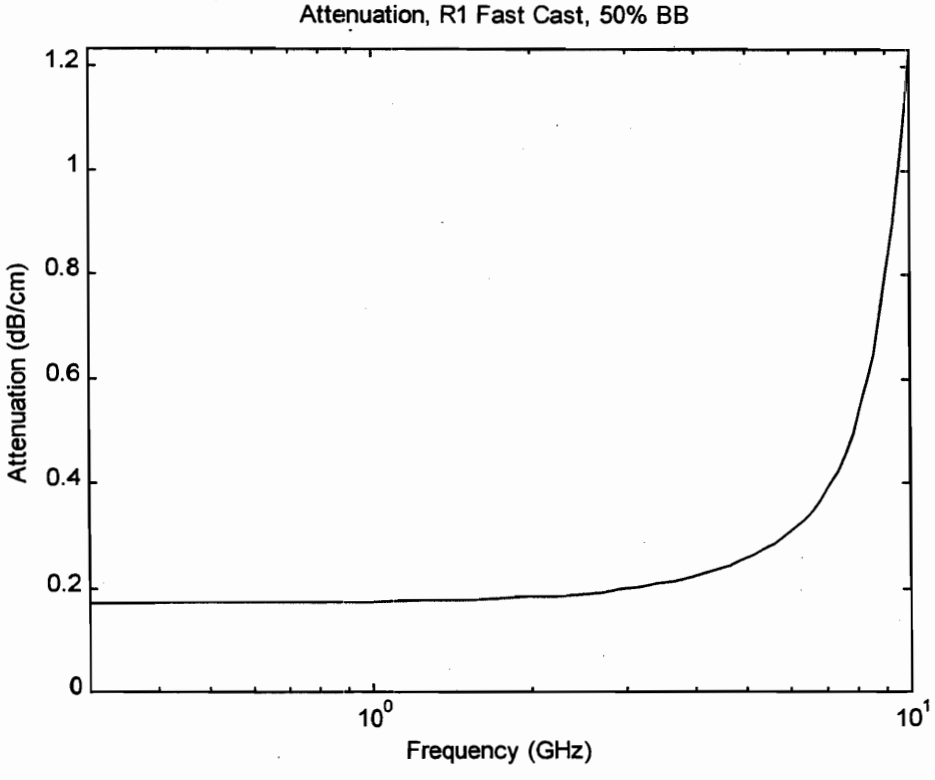

Figure 27. R1 Fast Cast with 50% BB filler, loss tangent and attenuation.

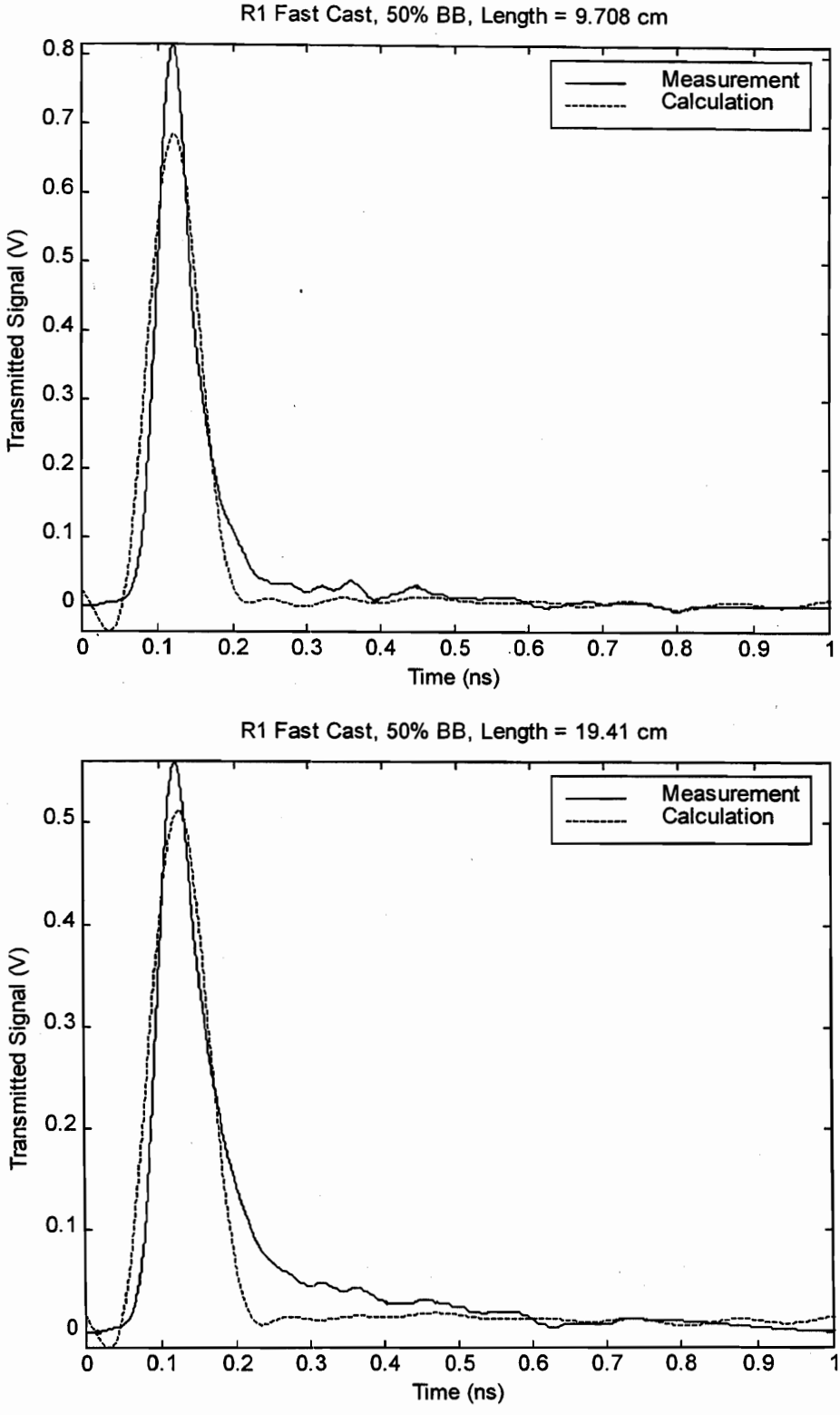

Figure 28. R1 Fast Cast with 50% BB filler, transmitted waveforms, measured and calculated. Calculated peak heights are somewhat low. As a result of the waveform truncation for processing, the late-time tails are not reproduced.

4.4.3. R1 Fast Cast, 50% Solid Glass Micro-sphere (HG3000) Filler

On the basis of signal transit time, we observed a dielectric constant in the range from 3.6 to 3.8. The signal processing of the transmitted waveforms produced 3.6 for the average real part of the complex permittivity over a range of 0.7 to 6 GHz. The loss tangent was 0.059 over the same frequency range. Transit times for measured and calculated impulse transmission data are essentially identical. The calculated peak heights are slightly low, indicating a possible over-estimate of the loss.

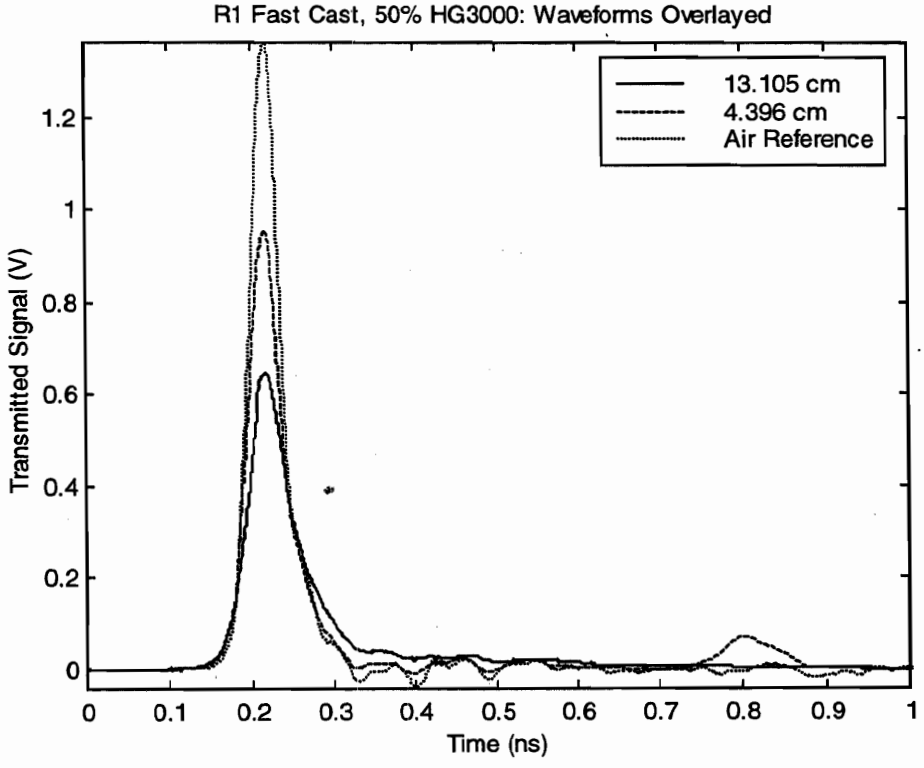

Figure 29. Overlay of waveforms transmitted through R1 Fast Cast containing 50% HG3000 filler with an air reference. For the short sample, the FWHM is 46 ps; for the long sample, we observe 57 ps. The measurements were truncated beyond 0.33 ns for processing.

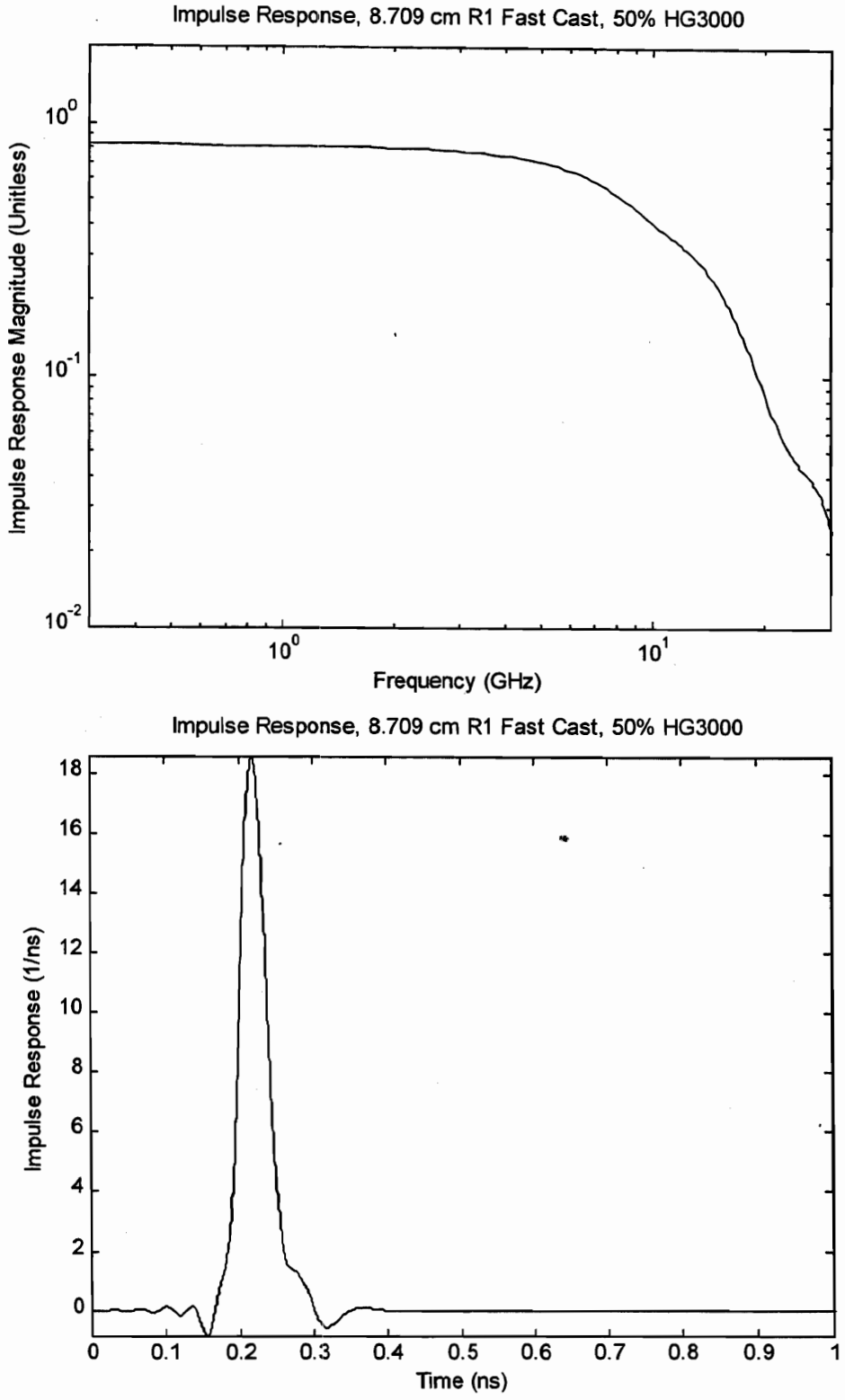

Figure 30. R1 Fast Cast with 50% HG3000 filler, impulse response. The signal processing employed a second order modified Butterworth filter at 14 GHz. The FWHM in the time domain is 41 ps.

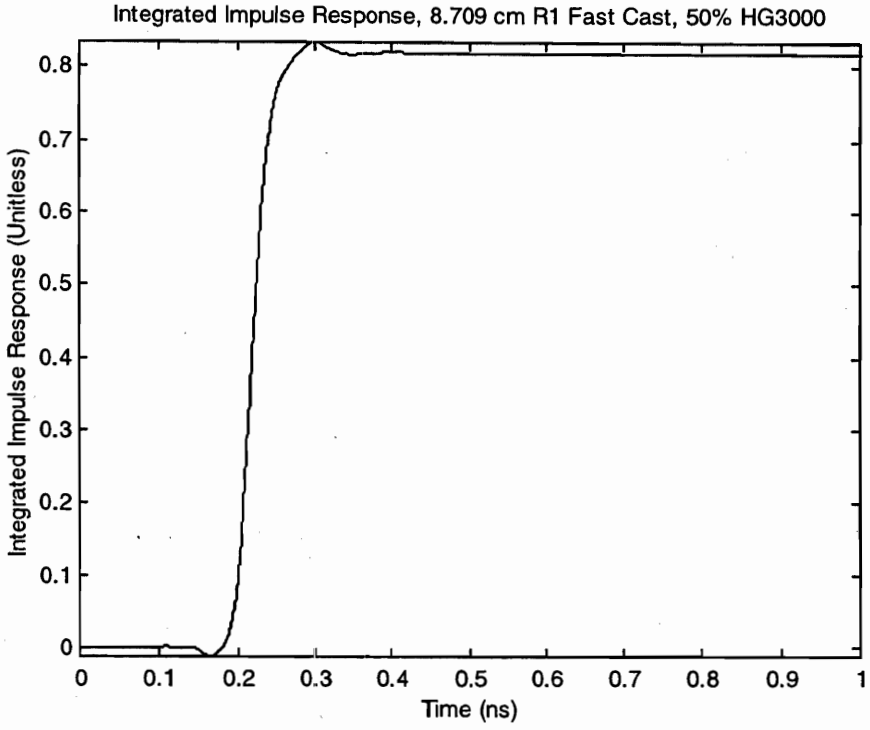

Figure 31. Integral of impulse response of R1 Fast Cast with 50% HG3000 filler. The rise time is 48 ps.

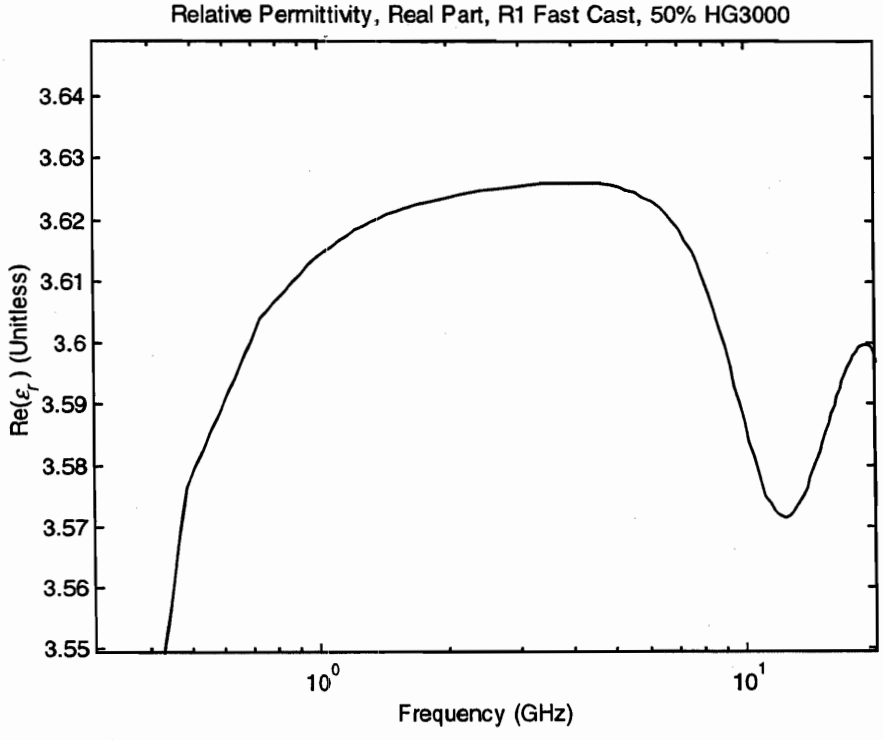

Figure 32. R1 Fast Cast with 50% HG3000 filler, real part of permittivity.

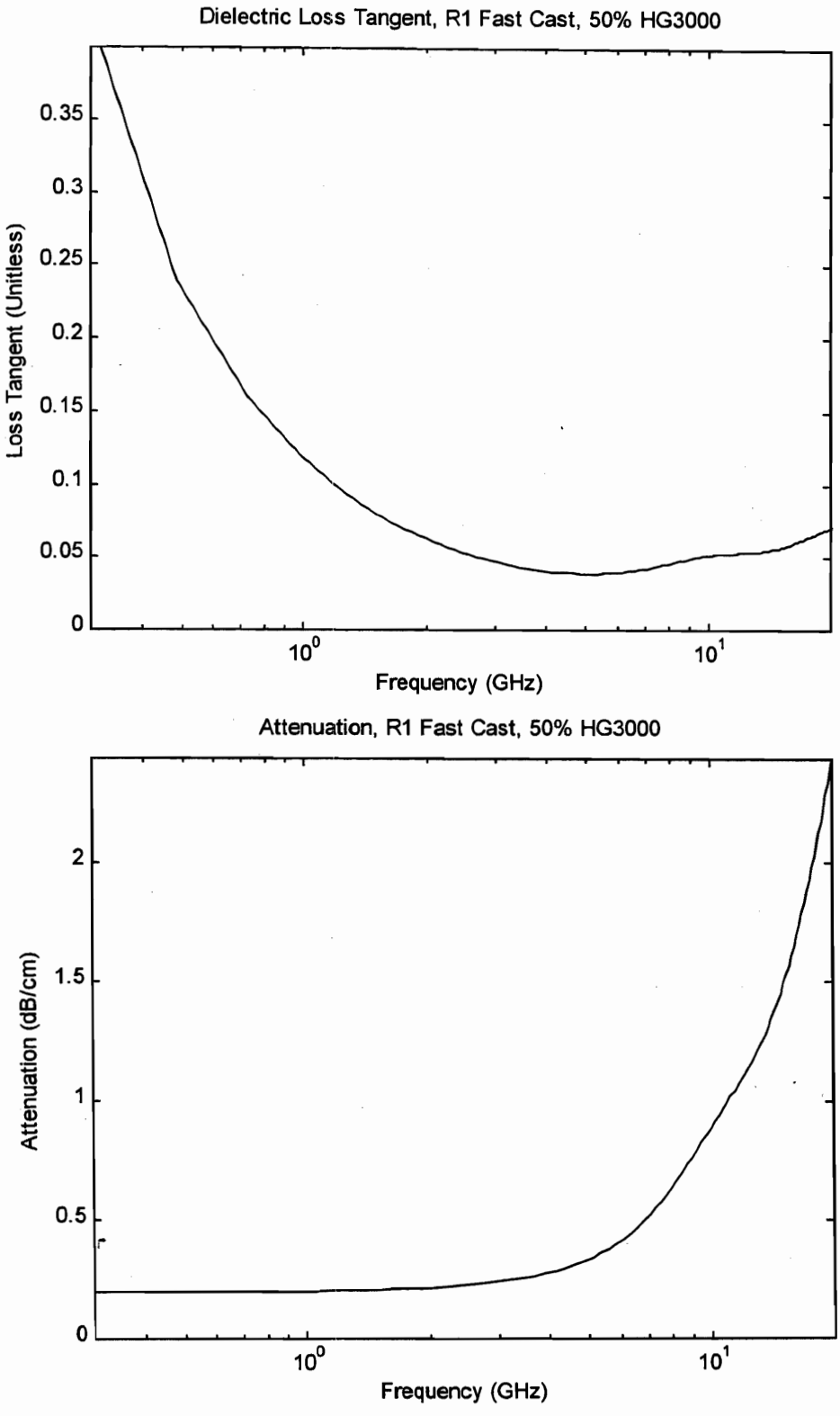

Figure 33. R1 Fast Cast with 50% HG3000 filler, loss tangent and attenuation.

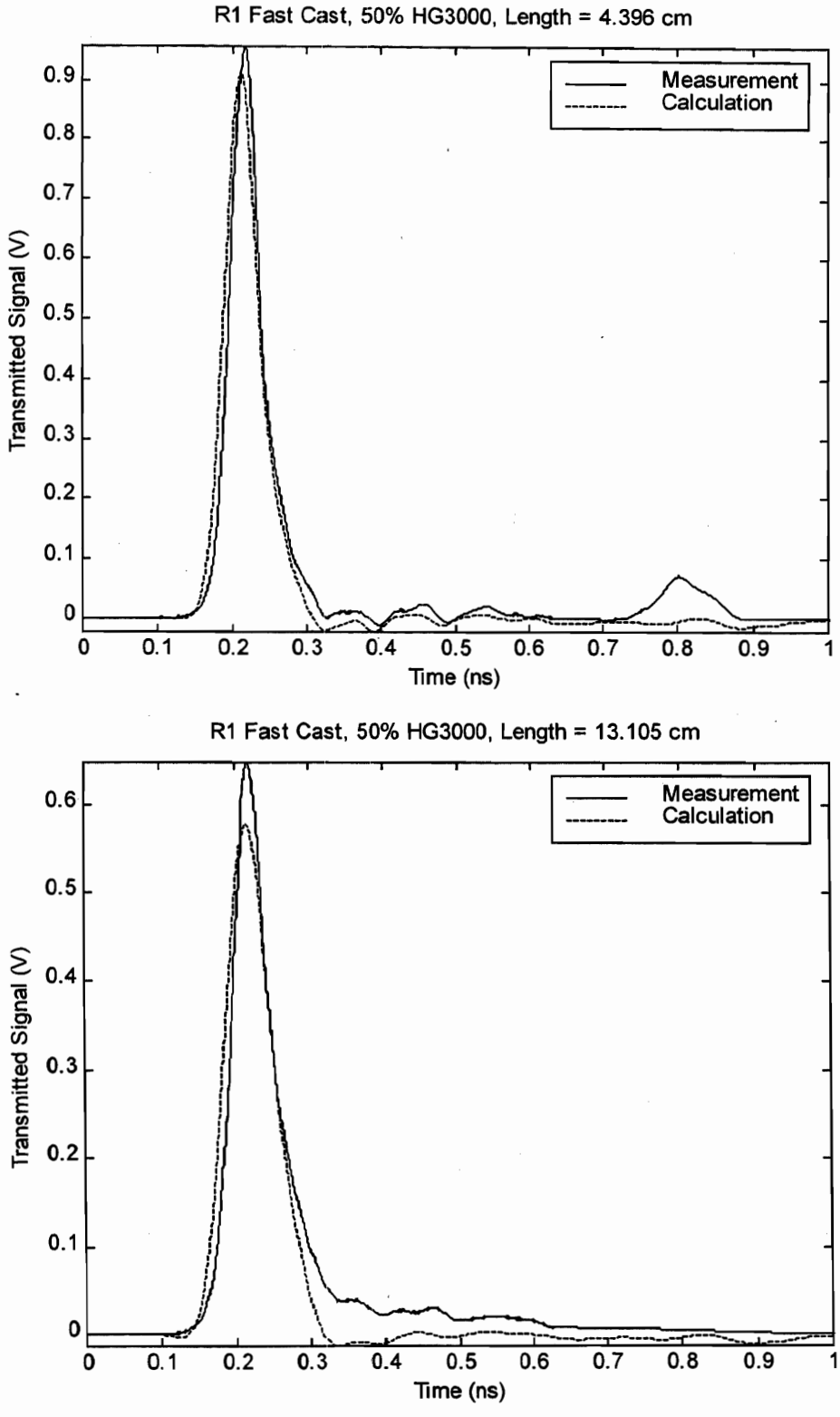

Figure 34. R1 Fast Cast with 50% HG3000 filler, transmitted waveforms, measured and calculated. Calculated peak heights are slightly low.

4.4.4. R1 Fast Cast, 5% Titanium Dioxide–Ethylene Glycol Pigment Dispersion

On the basis of signal transit time, we observed a dielectric constant in the range from 2.9 to 3.0. The signal processing of the transmitted waveforms produced 2.9 for the average real part of the complex permittivity over a range of 1 to 6 GHz. The loss tangent was 0.057 over the same frequency range. There are minor transit time differences between measured and calculated impulse transmission data; the calculated peaks arrive about 14 ps early. Also, the calculated peak heights are somewhat low, indicating a possible over-estimate of the loss.

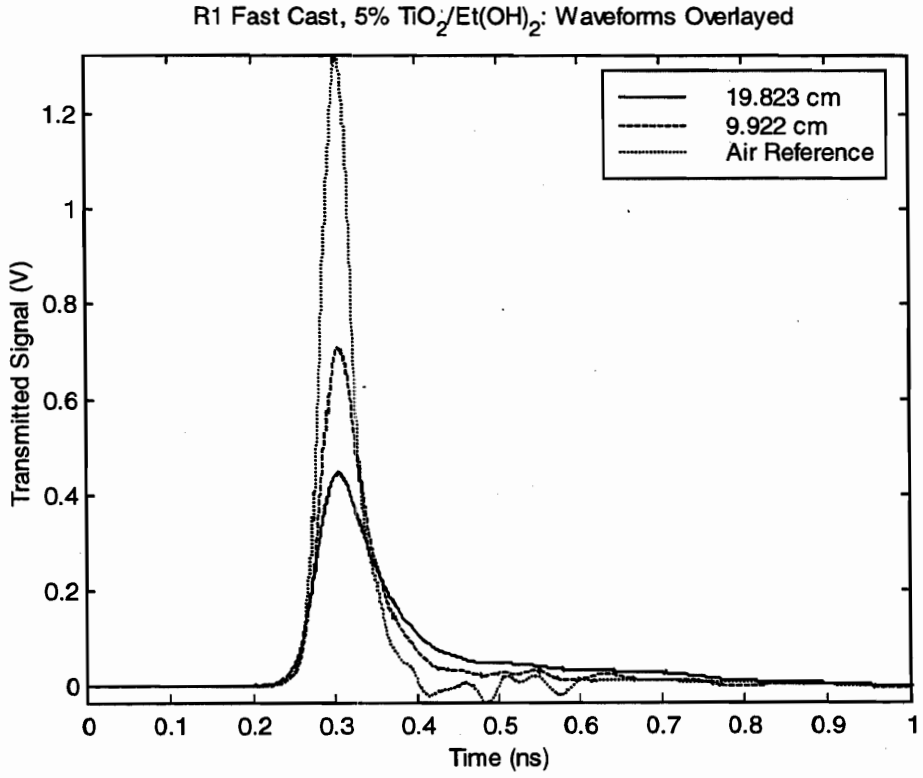

Figure 35. Overlay of waveforms transmitted through R1 Fast Cast containing 5% of a titanium dioxide/ethylene glycol dispersion with an air reference. For the short sample, the FWHM is 57 ps; for the long sample, we observe 82 ps. The measurements were truncated beyond 0.41 ns for processing.

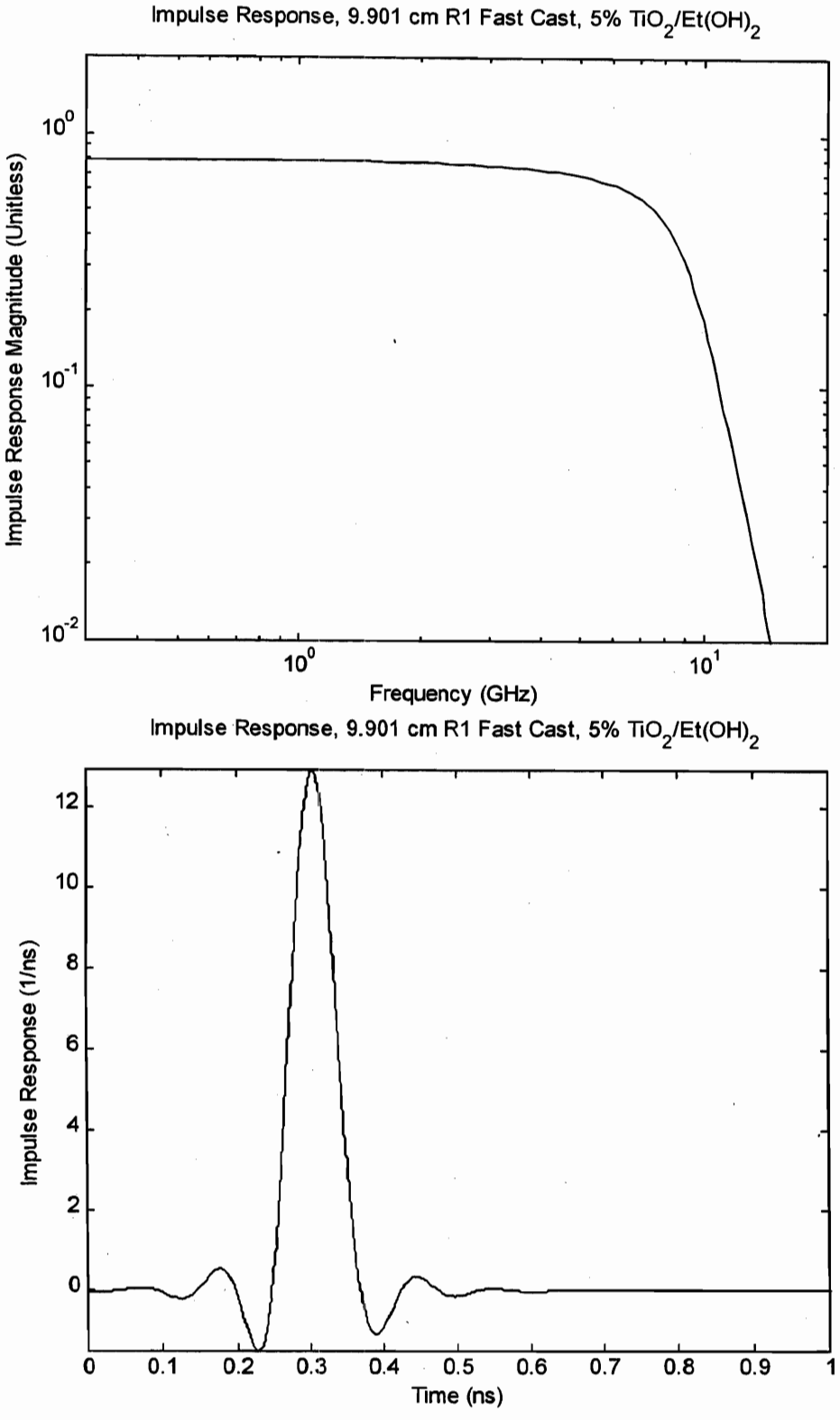

Figure 36. R1 Fast Cast with 5% titanium dioxide/ethylene glycol dispersion, impulse response. The signal processing employed a fifth order modified Butterworth filter at 10 GHz. The FWHM in the time domain is 66 ps.

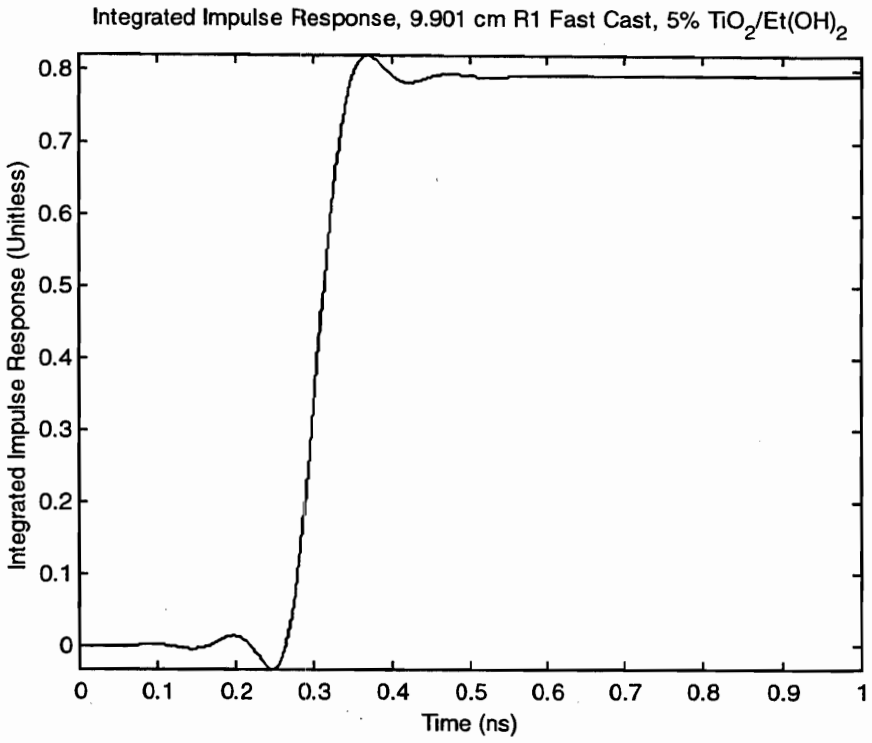

Figure 37. Integral of impulse response of R1 Fast Cast with 5% titanium dioxide/ethylene glycol dispersion. The rise time is 61 ps.

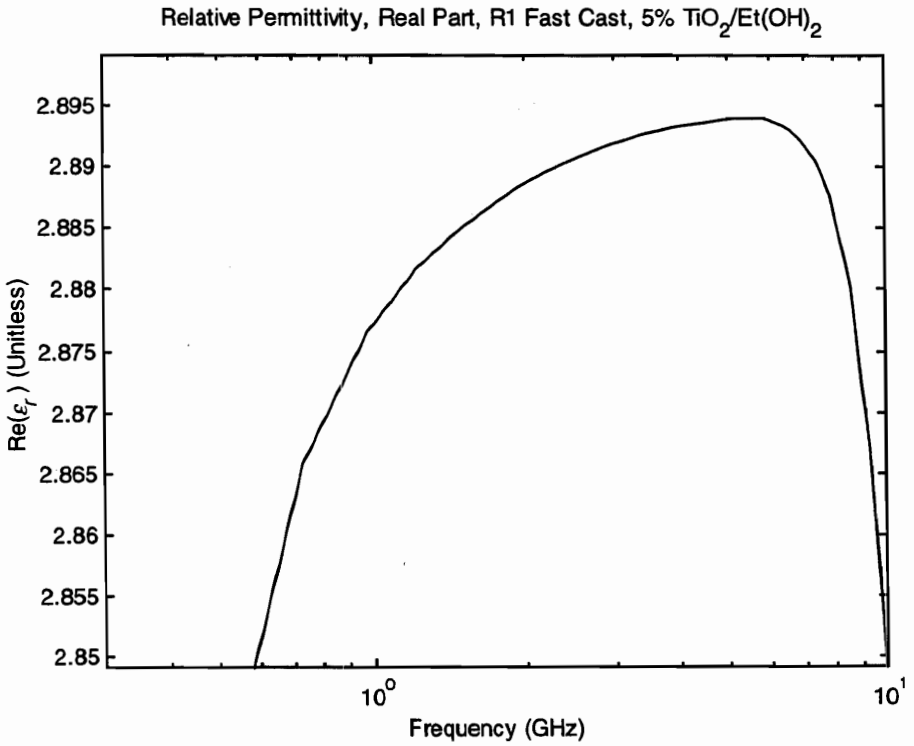

Figure 38. R1 Fast Cast with 5% titanium dioxide/ethylene glycol dispersion, real part of permittivity.

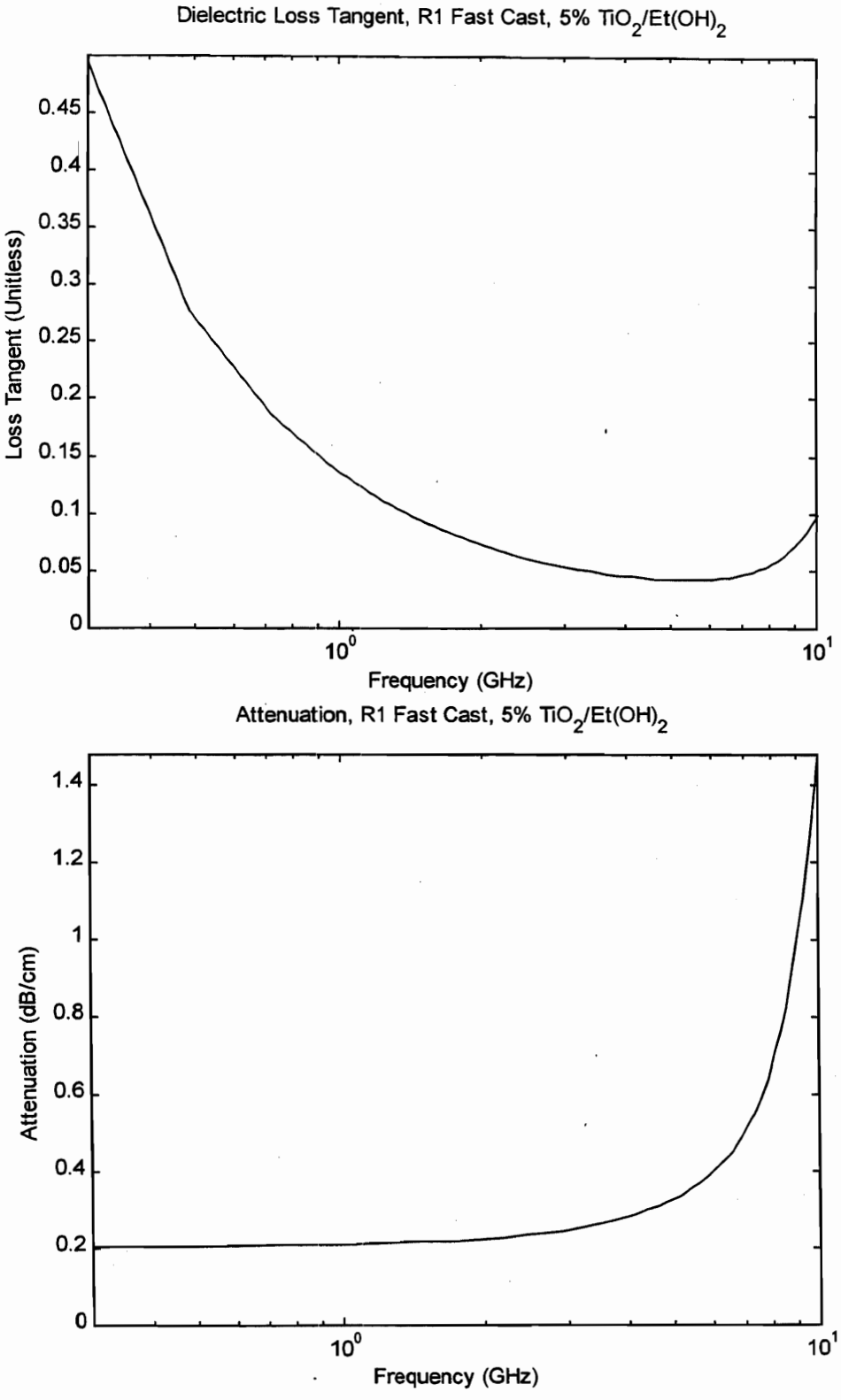

Figure 39. R1 Fast Cast with 5% titanium dioxide/ethylene glycol dispersion, loss tangent and attenuation.

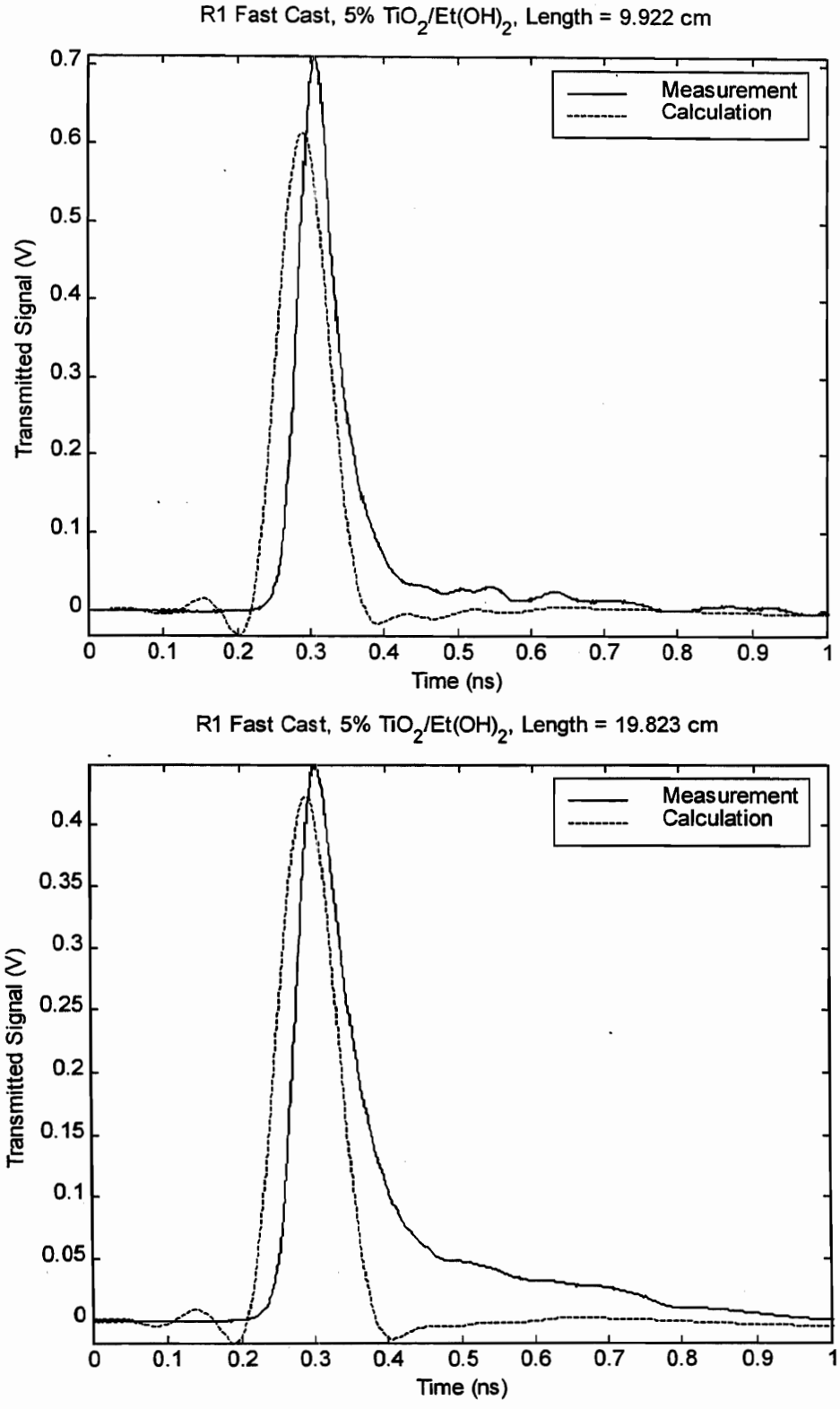

Figure 40. R1 Fast Cast with 5% titanium dioxide/ethylene glycol dispersion, transmitted waveforms, measured and calculated. Calculated transit times are short by only about 14 ps, and calculated peak heights are somewhat low. As a result of the waveform truncation for processing, the late-time tails are not reproduced well.

4.4.5. R1 Fast Cast, 25% Titanium Dioxide Filler

On the basis of signal transit time, we observed a dielectric constant in the range from 3.4 to 3.7. The signal processing of the transmitted waveforms produced 3.3 for the average real part of the complex permittivity over a range of 0.7 to 6 GHz. The loss tangent was 0.055 over the same frequency range. There are small transit time differences between measured and calculated impulse transmission data; the calculated peaks arrive about 33 ps early. The calculated peak heights are only slightly lower than their measured counterparts.

It must be noted that the samples measured here were heat-cured at 160°C for 24 hours to drive off apparently unreacted resin. This had the undesirable side effect of shrinking and warping the samples. As a result, there were air gaps between the samples and the conductors of the test fixture; and the data observed for these samples must be considered in that light.

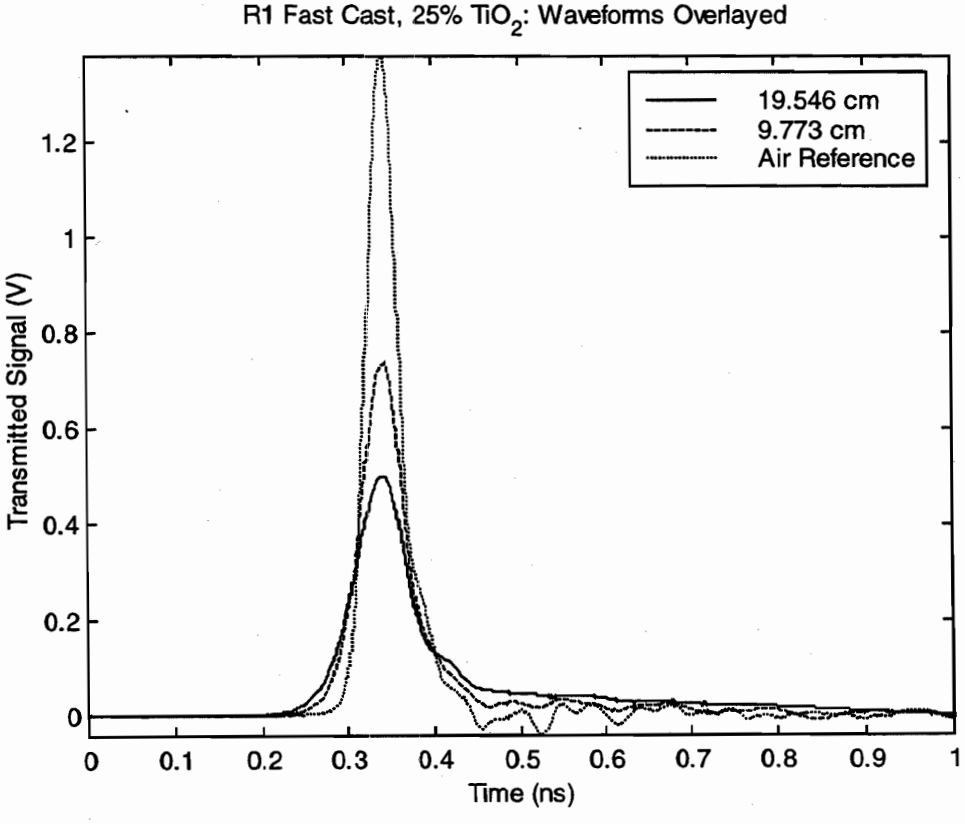

Figure 41. Overlay of waveforms transmitted through R1 Fast Cast containing 25% titanium dioxide filler with an air reference. For the short sample, the FWHM is 57 ps; for the long sample, we observe 71 ps. The measurements were truncated beyond 0.45 ns for processing.

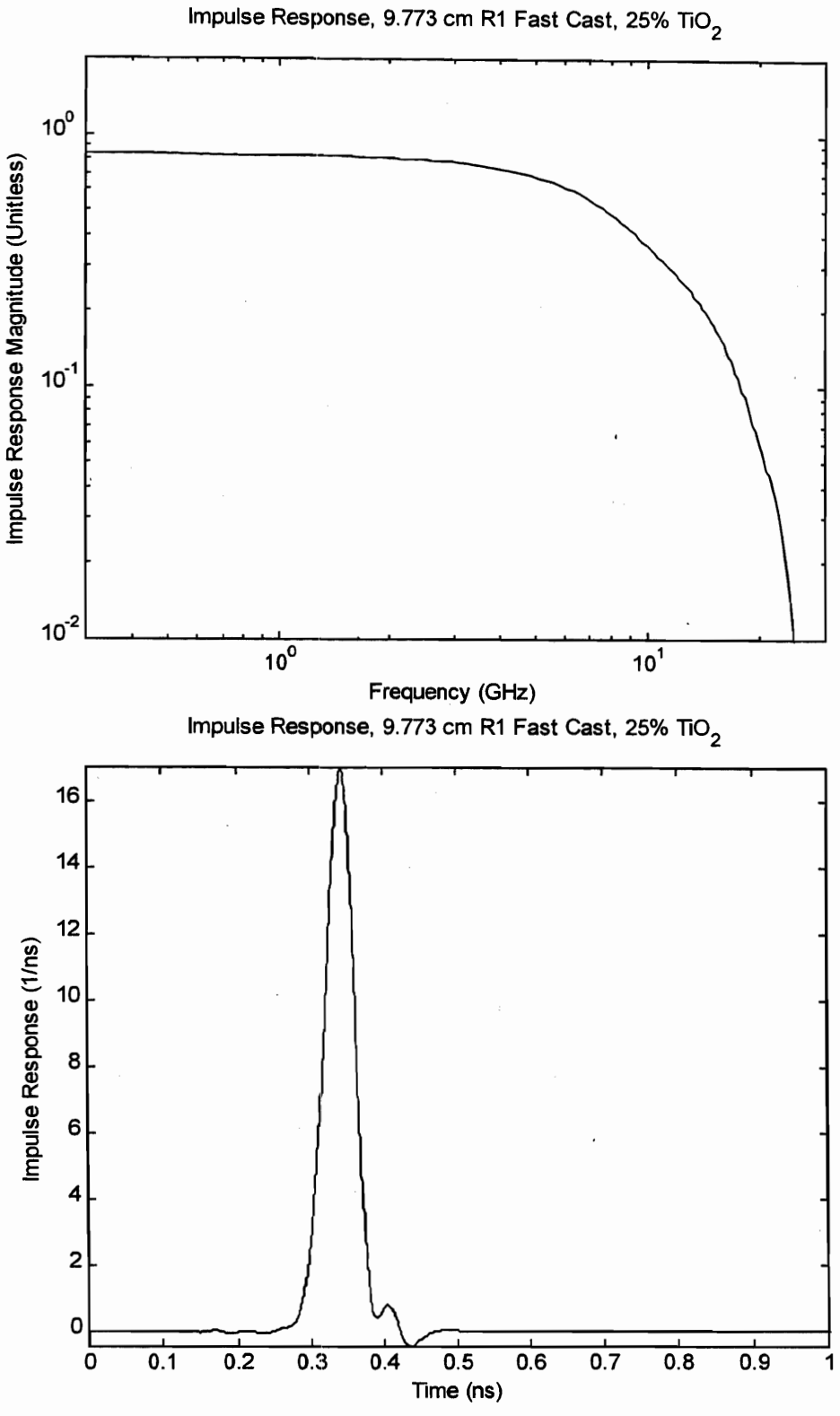

Figure 42. R1 Fast Cast with 25% titanium dioxide filler, impulse response. The signal processing employed a second order modified Butterworth filter at 14 GHz. The FWHM in the time domain is 46 ps.

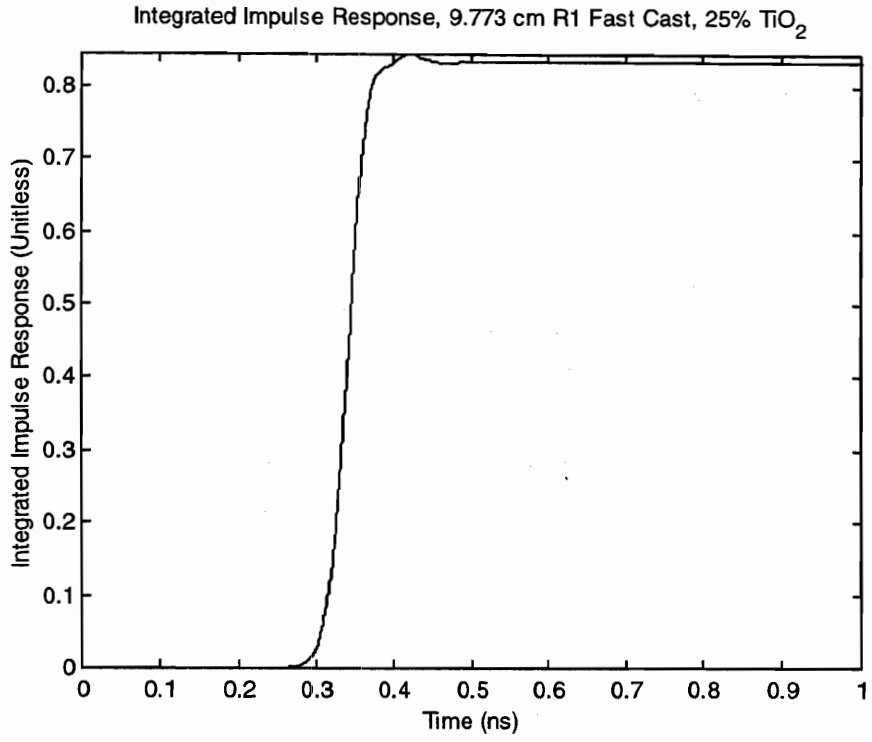

Figure 43. Integral of impulse response of R1 Fast Cast with 25% titanium dioxide filler. The rise time is 52 ps.

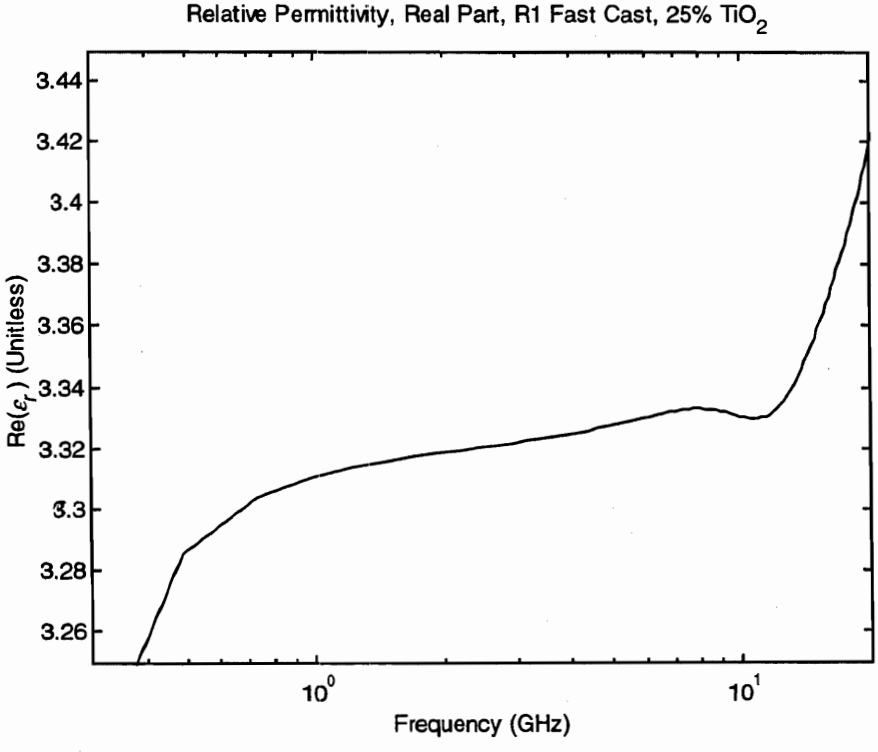

Figure 44. R1 Fast Cast with 25% titanium dioxide filler, real part of permittivity.

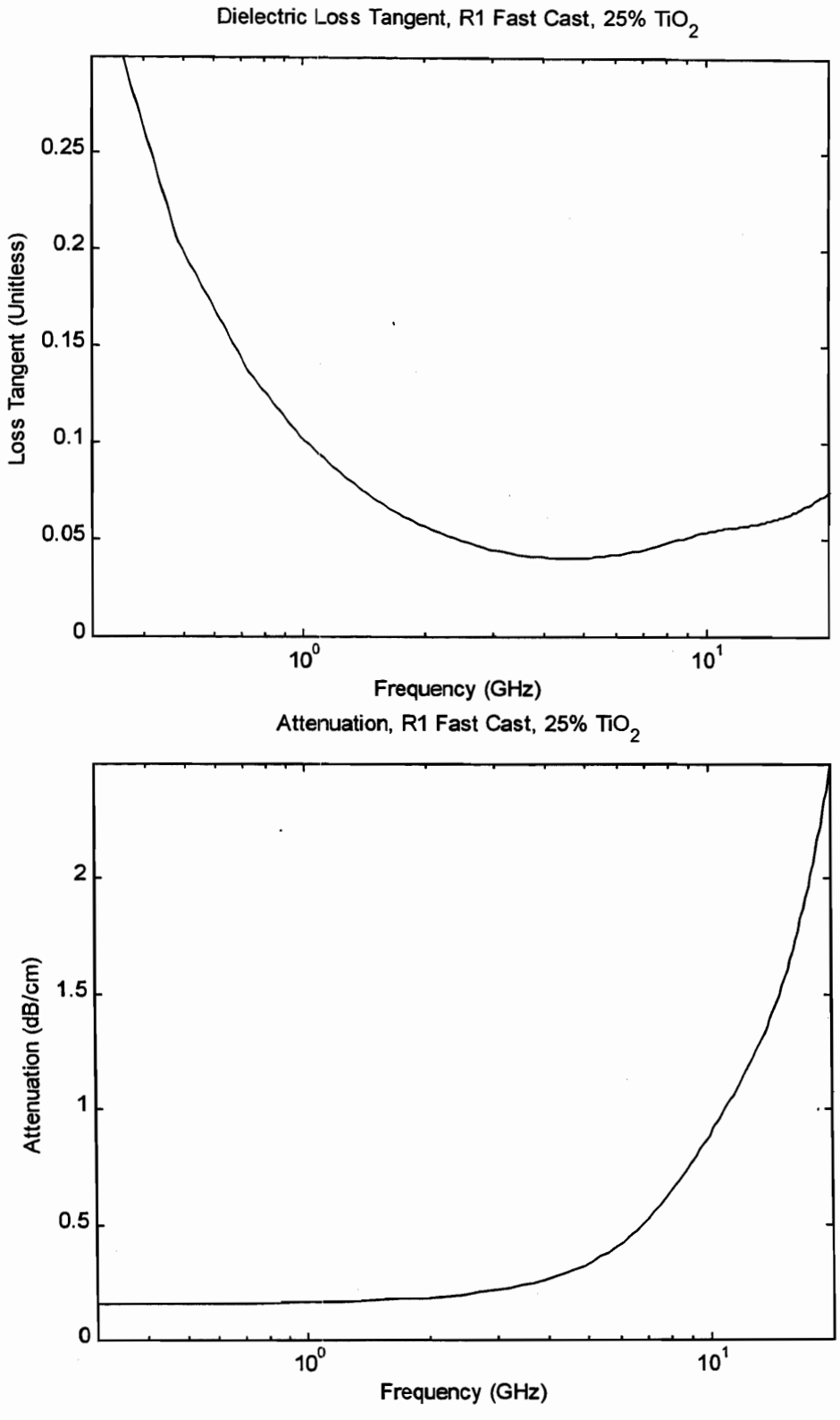

Figure 45. R1 Fast Cast with 25% titanium dioxide filler, loss tangent and attenuation.

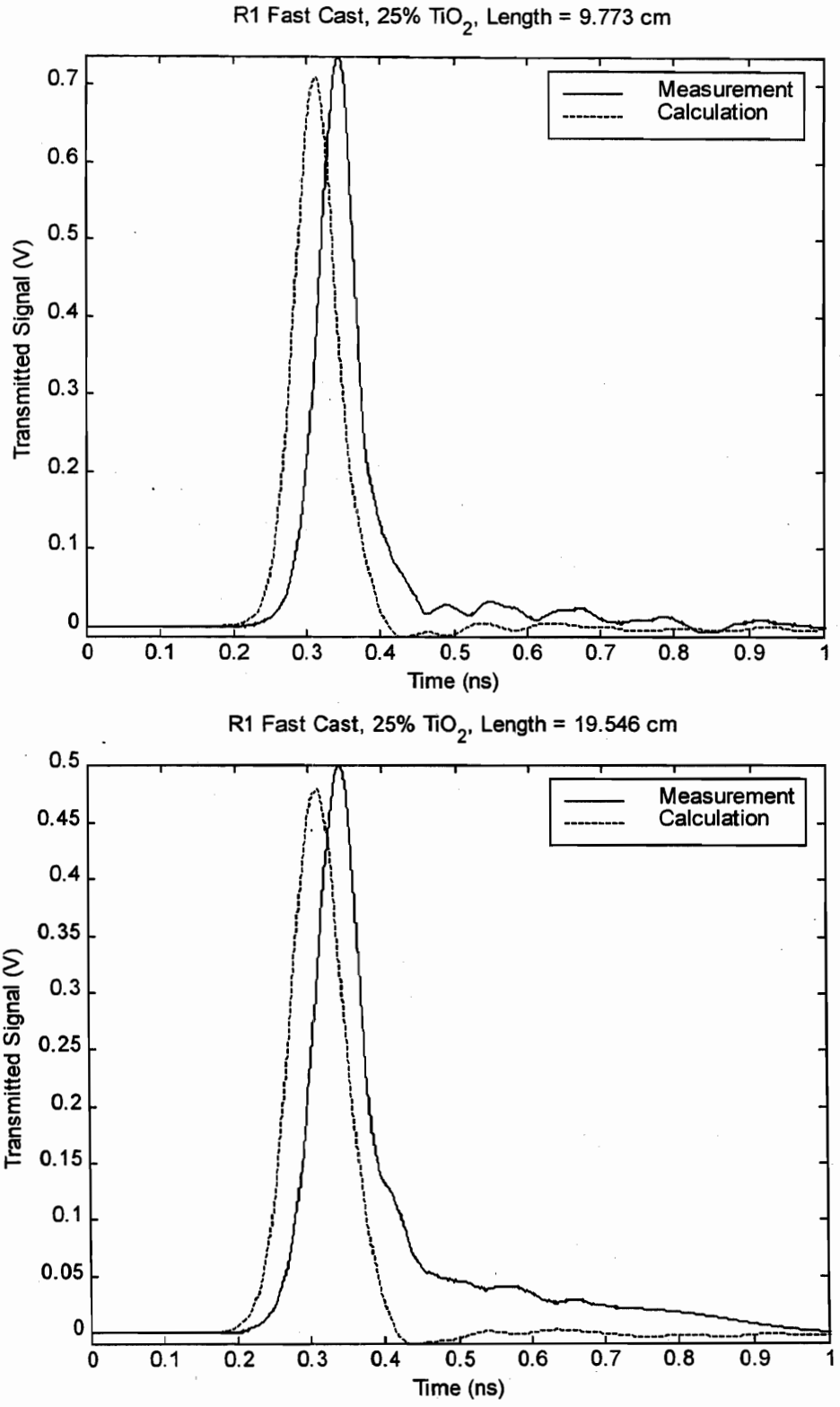

Figure 46. R1 Fast Cast with 25% titanium dioxide filler, transmitted waveforms, measured and calculated. Calculated transit times are short by about 35 ps, but calculated peak heights are only slightly low. As a result of the waveform truncation for processing, the late-time tails are not reproduced well.

4.4.6. R1 Fast Cast, 37% Titanium Dioxide Filler

On the basis of signal transit time, we observed a dielectric constant in the range from 3.6 to 4.3. The signal processing of the transmitted waveforms produced 3.6 for the average real part of the complex permittivity over a range of 0.7 to 6 GHz. The loss tangent was 0.053 over the same frequency range. There are transit time differences between measured and calculated impulse transmission data; the calculated peaks arrive about 55 ps early. Also, the calculated peak heights are somewhat high, indicating a possible under-estimate of the loss.

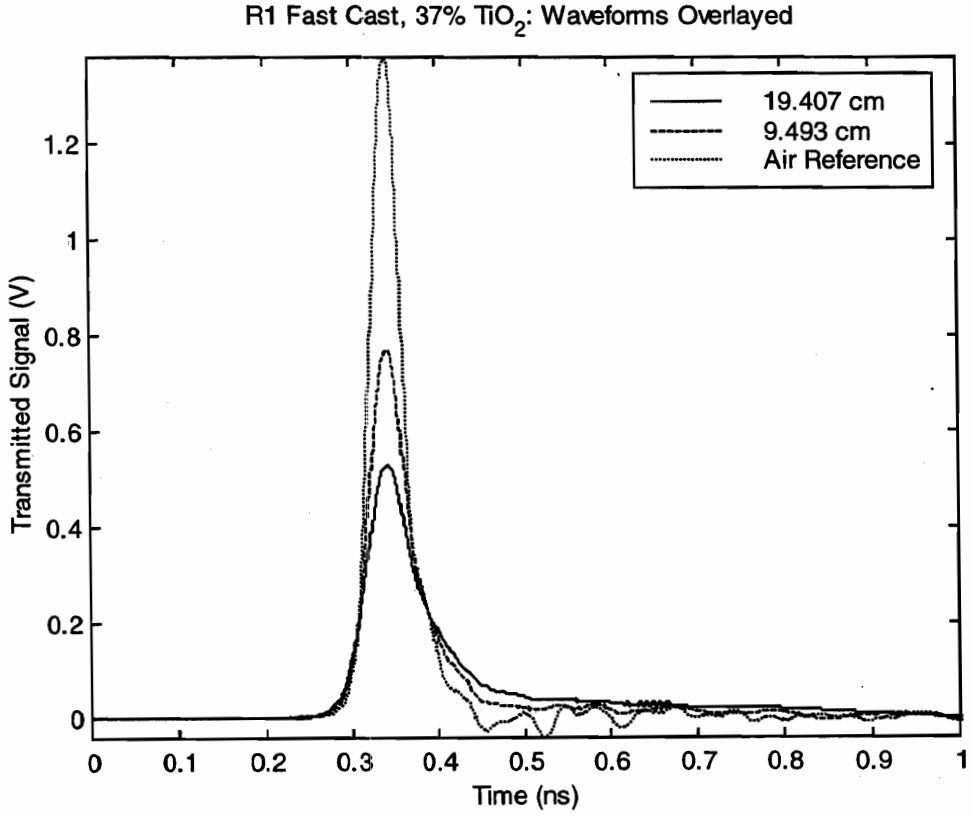

Figure 47. Overlay of waveforms transmitted through R1 Fast Cast containing 37% titanium dioxide filler with an air reference. For the short sample, the FWHM is 53 ps; for the long sample, we observe 66 ps. The measurements were truncated beyond 0.44 ns for processing.

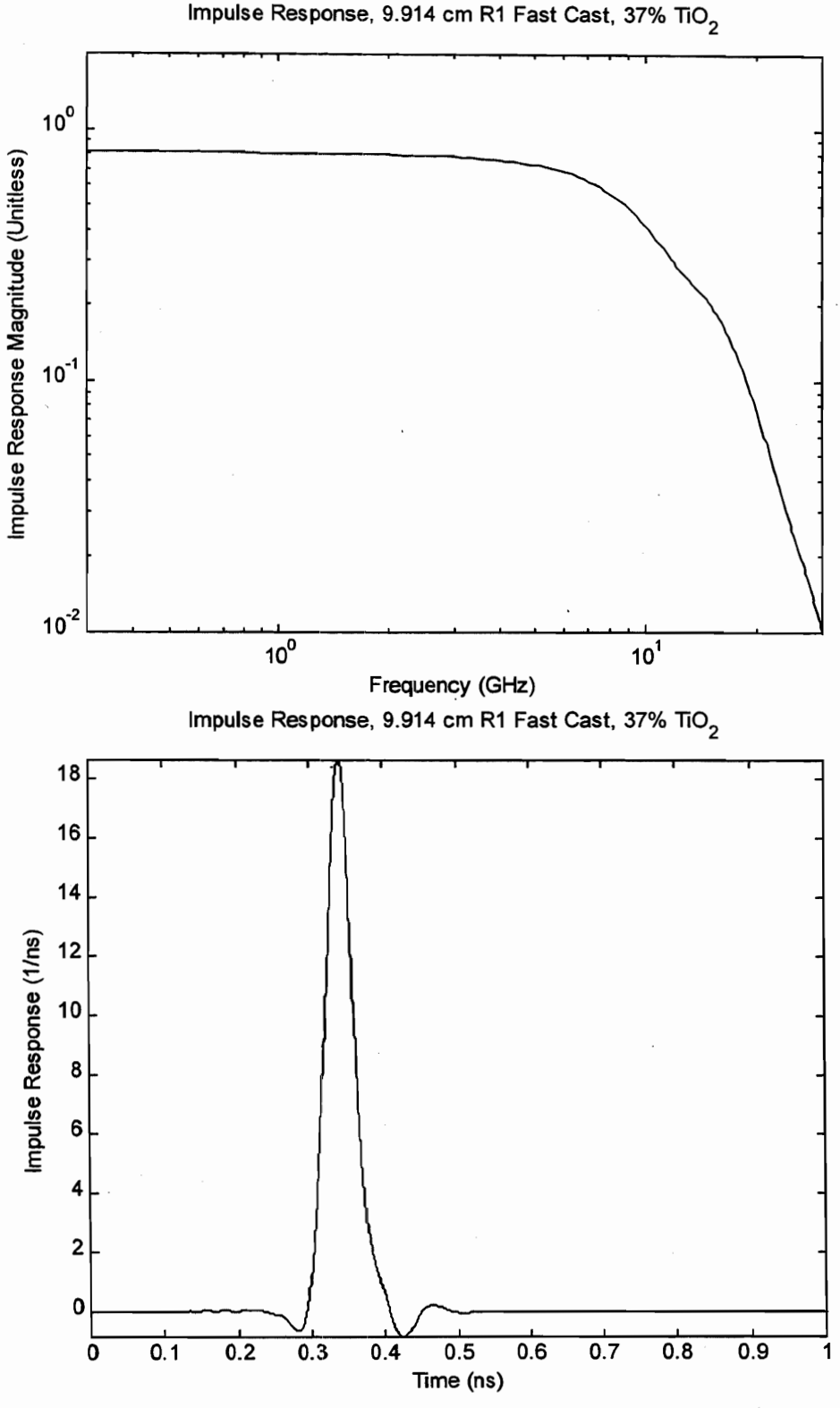

Figure 48. R1 Fast Cast with 37% titanium dioxide filler, impulse response. The signal processing employed a second order modified Butterworth filter at 14 GHz. The FWHM in the time domain is 41 ps.

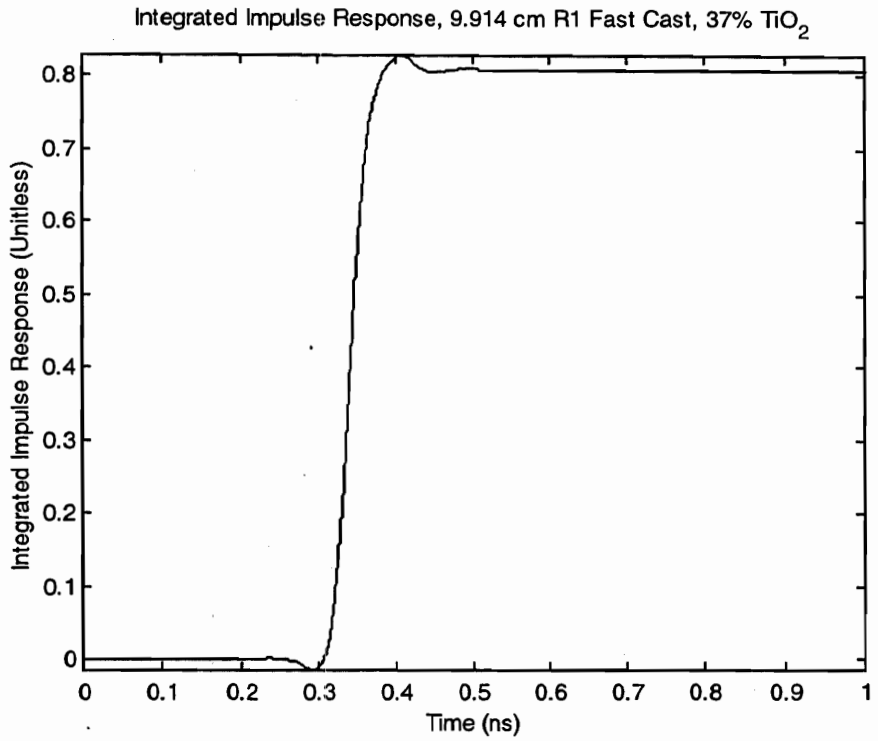

Figure 49. Integral of impulse response of R1 Fast Cast with 37% titanium dioxide filler. The rise time is 47 ps.

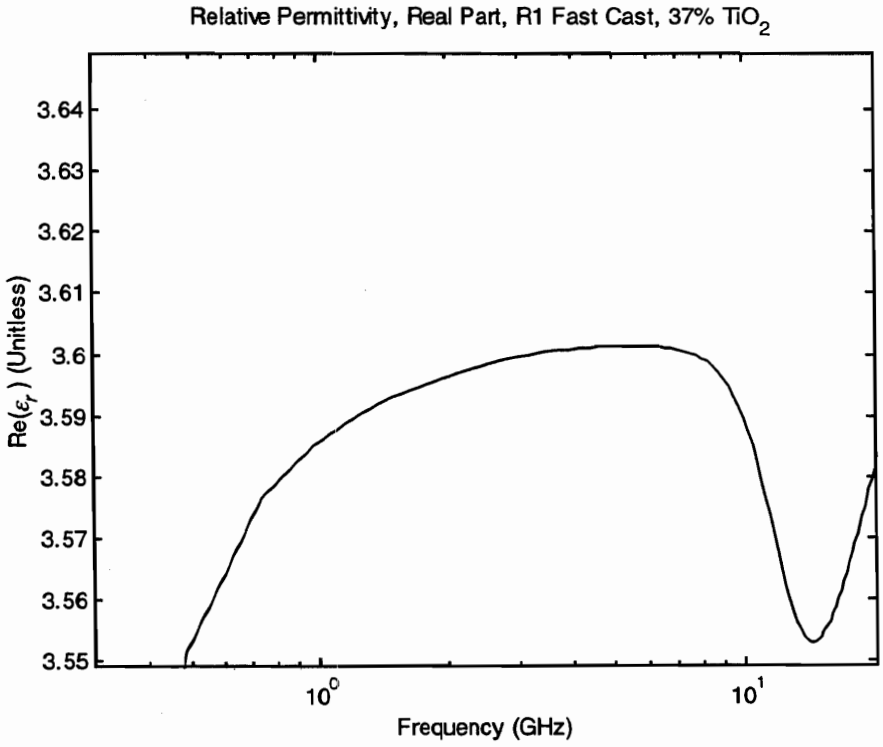

Figure 50. R1 Fast Cast with 37% titanium dioxide filler, real part of permittivity.

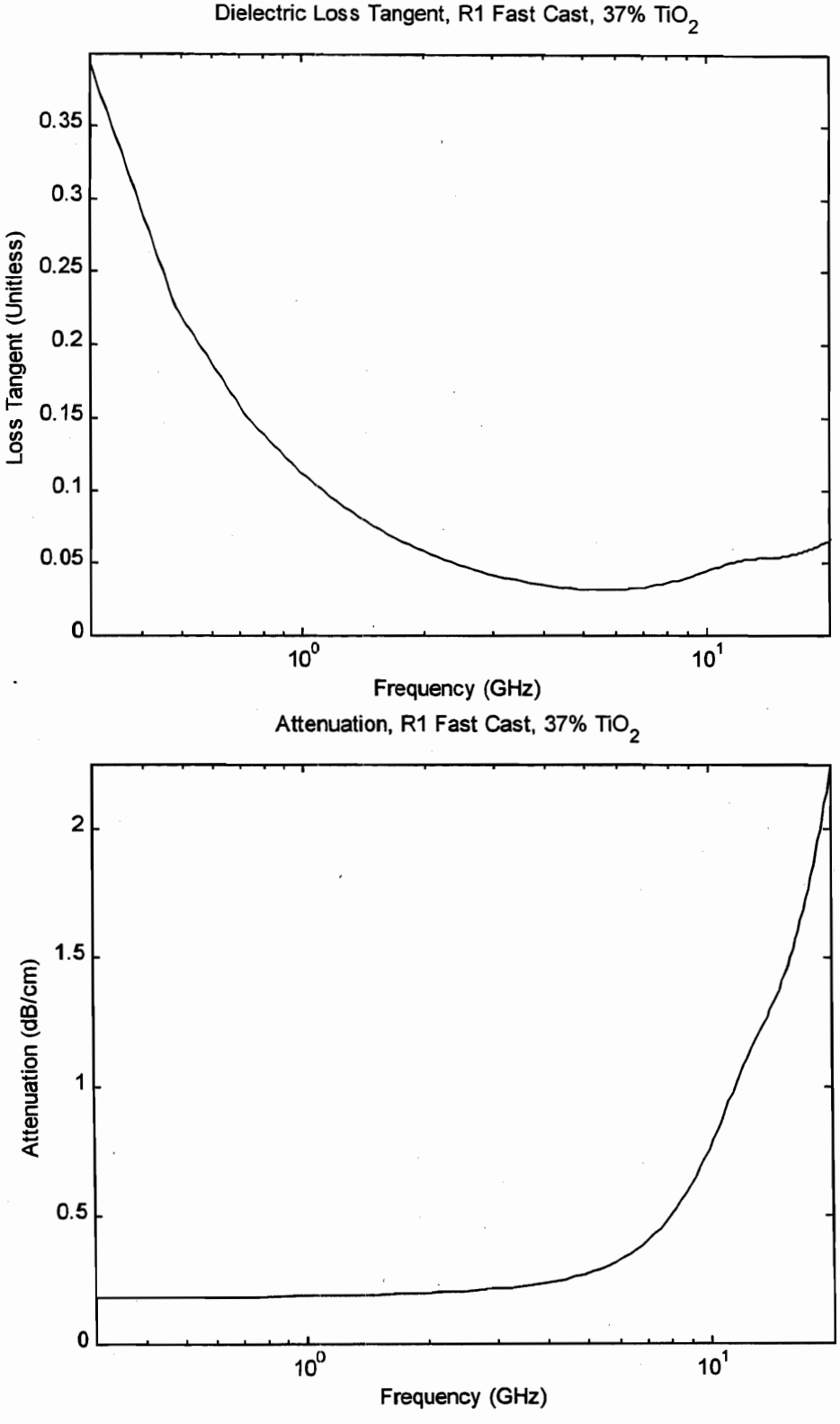

Figure 51. R1 Fast Cast with 37% titanium dioxide filler, loss tangent and attenuation.

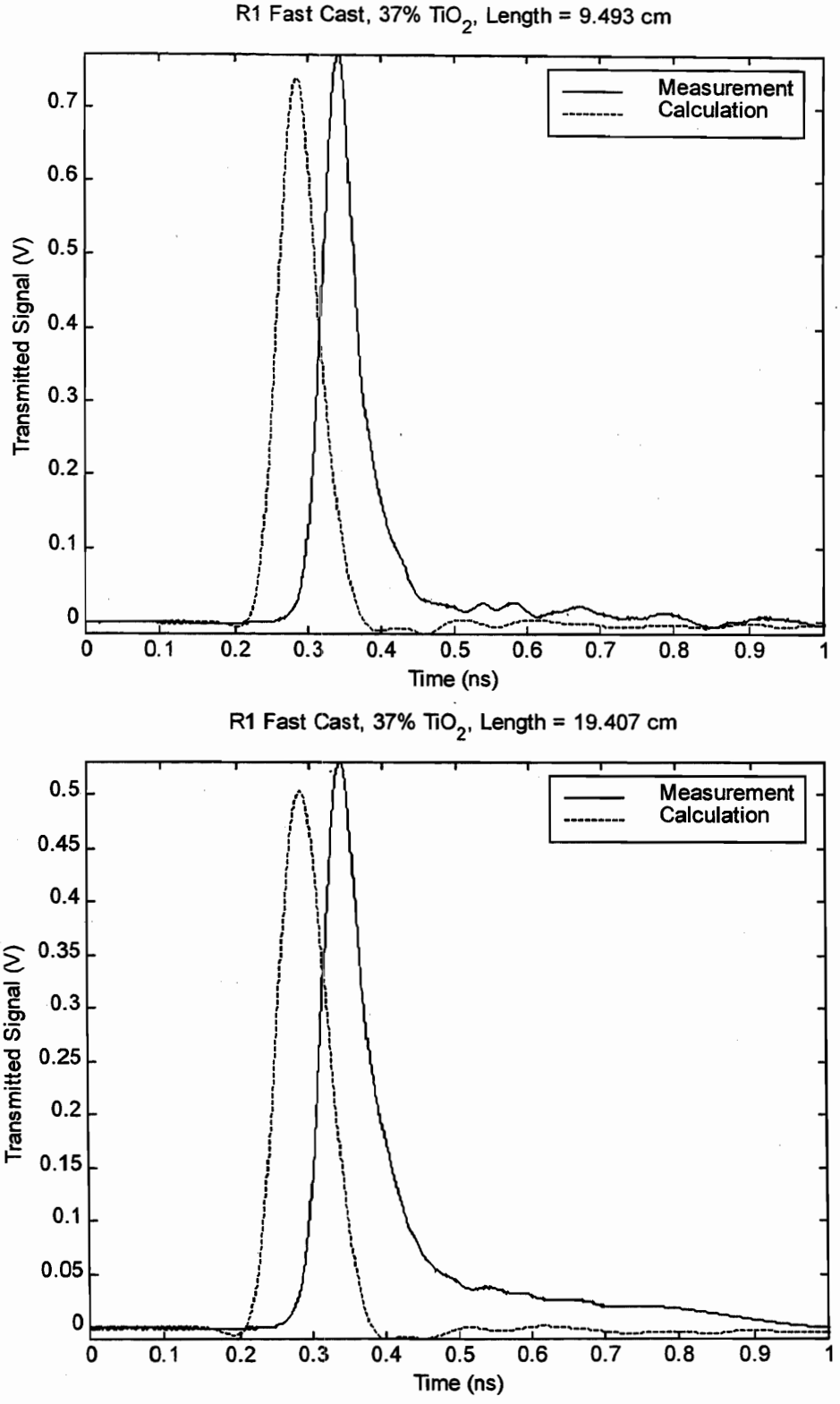

Figure 52. R1 Fast Cast with 37% titanium dioxide filler, transmitted waveforms, measured and calculated. Calculated transit times are short by about 55 ps, but calculated peak heights are only slightly low. As a result of the waveform truncation for processing, the late-time tails are not reproduced well.

5. Conclusion

We have built a 50 Ω TEM transmission line test fixture for making time domain measurements of the complex permittivity of solid dielectric materials. The fixture has a rectangular outer conductor cross section and a center conducting strip with fully rounded edges. Its sample chamber accommodates samples with a cross section of 2.3 × 6 cm and length up to 20 cm.

We used the test fixture to measure the complex permittivity of polymeric resins with potential application in construction of graded-layer dielectric transmission line bends. These materials included a polystyrene loaded with titanium dioxide and several polyurethane formulations, some with varying quantities of titanium dioxide loading. As a reference, we also measured UHMW polyethylene. We were successful in measuring the complex permittivity of the polyurethanes with a bandwidth extending from below 1 GHz to around 10 GHz. Although we were able to measure the real part of the permittivity of the polystyrene and polyethylene, the loss factors of these two materials were at or below the sensitivity of our measurements. For the polystyrene, the measured loss was more than six times larger than the manufacturer's asserted value; and our validation calculations suggested that our measurement over-estimated the loss. For the polyethylene, the measured loss was negative at all frequencies below about 6 GHz. This non-physical result indicates a loss very near zero and a measurement dominated by low-level noise.

Although our measurements were sufficiently sensitive to measure the loss factors of the polyurethanes, the attenuation of these materials is greater than desirable for our graded-layer transmission line application. For most formulations, the attenuation of the polyurethane samples exceeded 0.2 dB/cm over the measured frequency range. Moreover, the intrinsic rise times are nearly double those for the polystyrene and polyethylene samples. An additional problem with the polyurethane samples was our inability to achieve a useful dielectric constant range by varying the titanium dioxide loading. Although this problem might be surmountable by use of sophisticated mixing and casting techniques, the poor loss and rise time characteristics of the polyurethanes suggest that polystyrenes or other base materials with similar dielectric properties would be better suited to our application.

The sensitivity of our approach for measuring the complex permittivity of low-loss dielectrics could be improved somewhat by use of larger sample length differences. For example, instead of using sample sets consisting of two nearly equal lengths of material, sets with one very short length and one much longer length could be used. Additionally, the length could effectively

be doubled by measuring impulses after a round trip through the fixture, having reflected from a short at the far end. By employing both of these techniques, the propagation length could be almost quadrupled. Of course, a test fixture with a larger sample chamber could be built. However, since this measurement approach is essentially a destructive one, and many of the dielectric materials of interest are expensive, the pursuit of ever longer transmission line devices does not seem reasonable. For truly low-loss materials, the cavity resonance method, employed at a few fixed frequencies, is probably the preferred approach. Nevertheless, for high-loss dielectrics, the impulse transmission method has proven to be a quick and effective way to obtain extremely broadband complex permittivity data.

We can summarize our conclusions by observing that the transmission line measurement technique performs reasonably well for high-loss dielectric materials. However, such materials are not desirable for our graded-layer transmission line bend application. The search for appropriate materials should focus on ones like the polystyrenes, which are known to have low loss and to be amenable to dielectric property adjustment by loading with a high-dielectric-constant material.

Acknowledgment

We wish to thank William D. Prather, of the Air Force Research Laboratory, Directed Energy Directorate, for funding this work. We also wish to thank Dr. Carl E. Baum, also of the Air Force Research Laboratory, Directed Energy Directorate, for helpful discussions on this topic.

References

1 W. S. Bigelow and E. G. Farr, *Minimizing Dispersion in a TEM Waveguide Bend by a Layered Approximation of a Graded Dielectric Material*, Sensor and Simulation Note 416, 5 January 1998.

2 W. S. Bigelow and E. G. Farr, *Impedance of an Azimuthal TEM Waveguide Bend in a Graded Dielectric Medium*, Sensor and Simulation Note 428, 21 November 1998.

3 E. G. Farr and C. A. Frost, *Time Domain Measurement of the Dielectric Properties of Water in a Coaxial Test Fixture*, Measurement Note 49, December 1996.

4 E. G. Farr and C. A. Frost, *Impulse Propagation Measurements of the Dielectric Properties of Water, Dry Sand, Moist Sand, and Concrete*, Measurement Note 52, November 1997.